

Earth Science

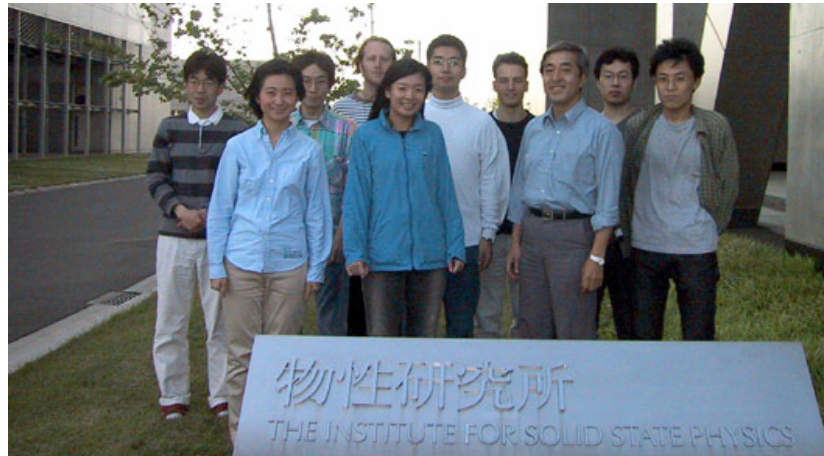
Takehiko Yagi

Geochemical Research Center (GCRC), University of Tokyo

Acknowledgments

I had been a heavy user of synchrotron radiations (PF and SPring-8) for these more than 35 years to do high P-T X-ray diffractions.

1971 – 2012 : Institute for Solid State Physics, Univ. Tokyo



2012 – 2014: Geodynamic Research Center, Ehime Univ.

2014 – present : Geochemical Research Center, Univ. Tokyo

Outline

Introduction

Materials under pressure

Earth's interior viewed by seismic wave

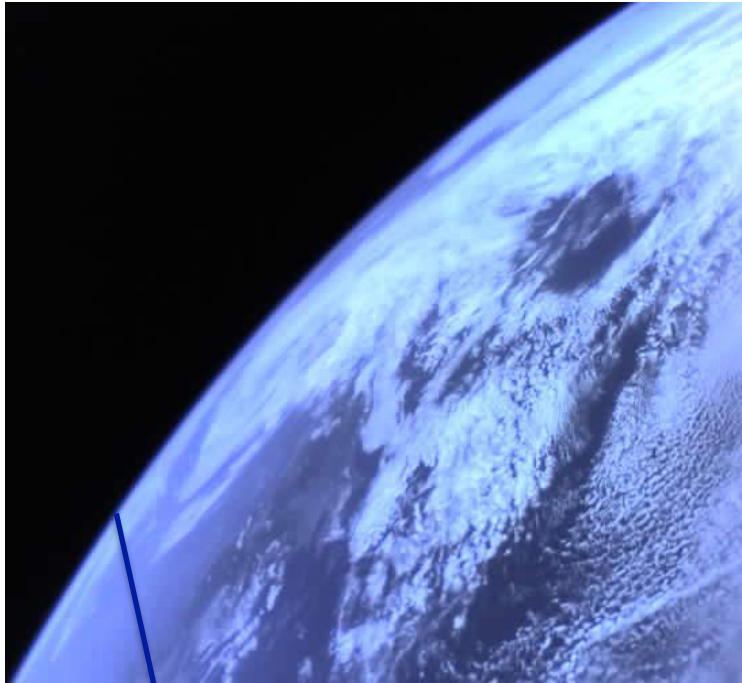
High-pressure experiments on minerals

High-density minerals discovered by these experiments

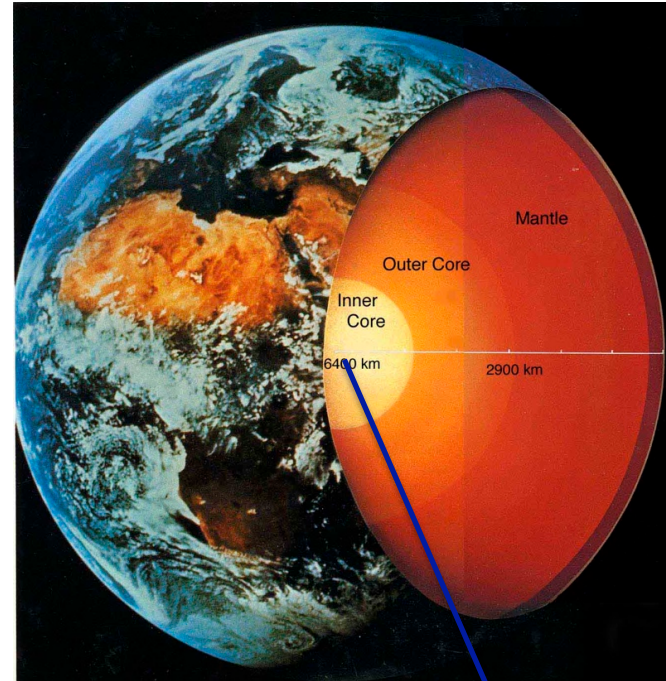
Present view of the dynamic Earth

Application to the study of novel materials

Pressures in the universe



1 atm (0.1 MPa)



360 GPa

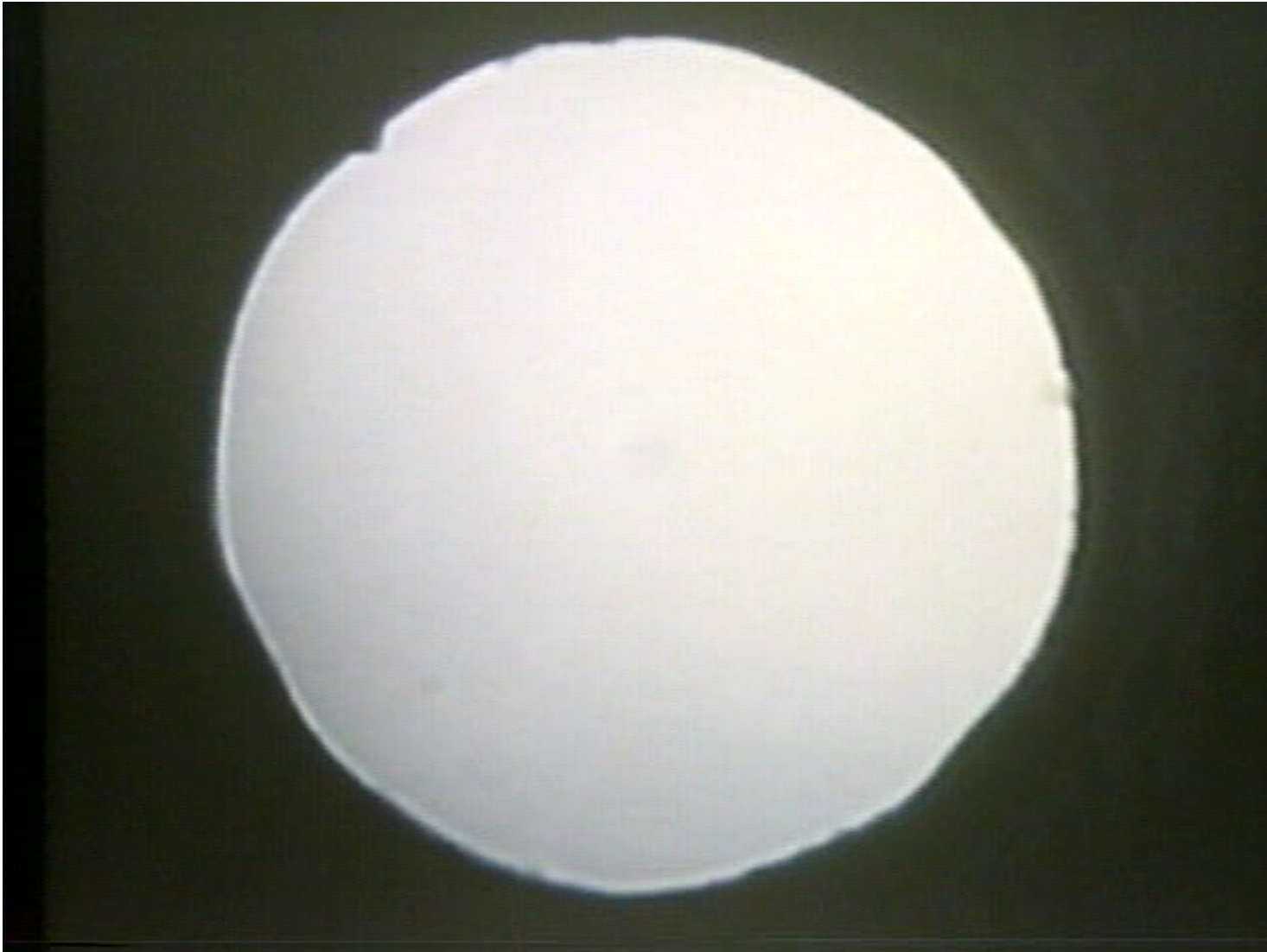
Bottom of the deepest sea: 0.1 GPa

Center of the Earth: 360 GPa

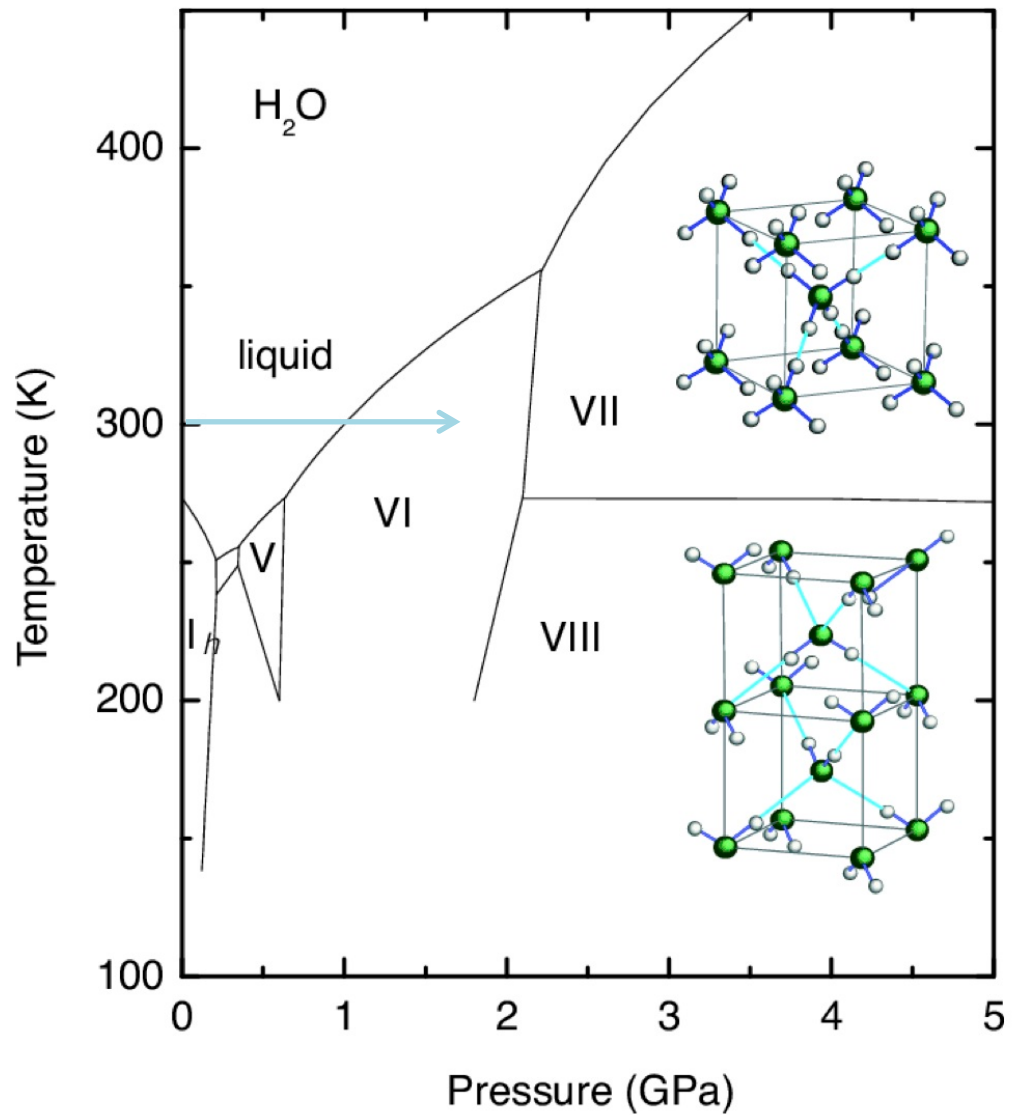
Center of Jupiter: 4.5 TPa (10^{12} Pa)

Center of the sun: 2.4×10^{16} Pa

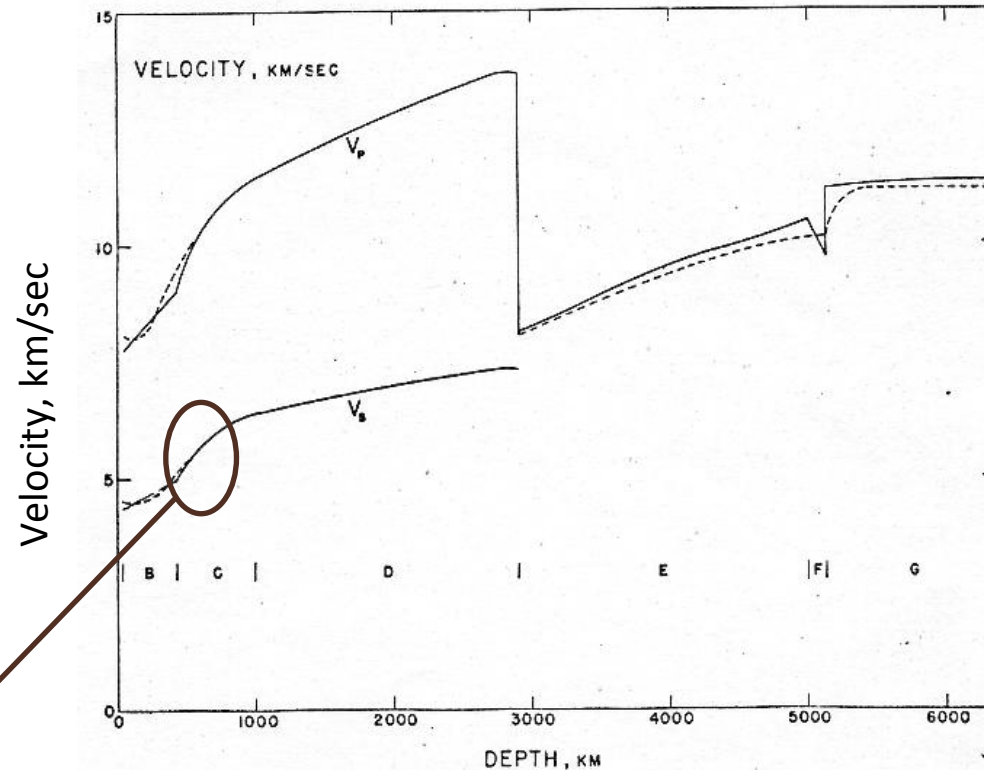
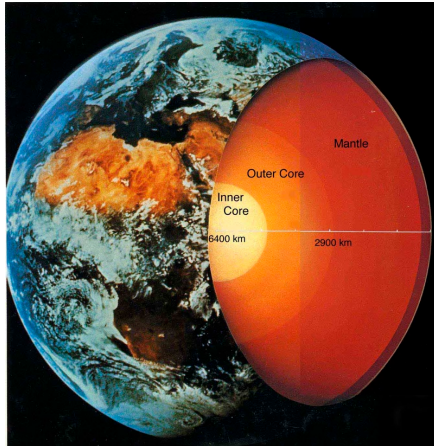
Behavior of H₂O at 300 K & high pressure



Phase diagram of H₂O ice



Earth's interior observed by seismology



“transition zone”

Depth, km

F. Birch (1952)

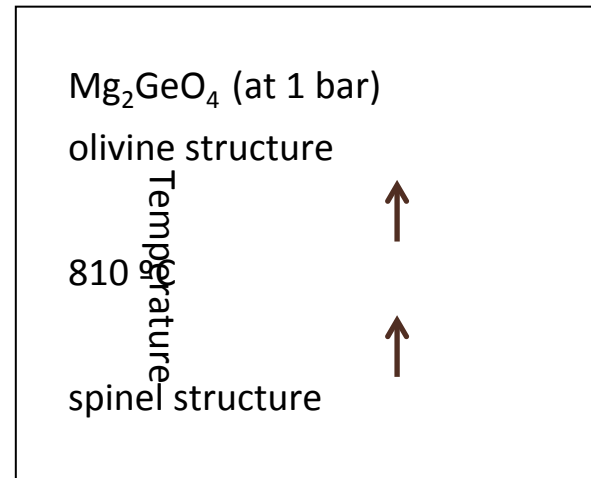
“Elasticity and constitution of the Earth's interior”

Most abundant mineral in the upper mantle

Olivine: $(\text{Mg,Fe})_2\text{SiO}_4$



“peridot”



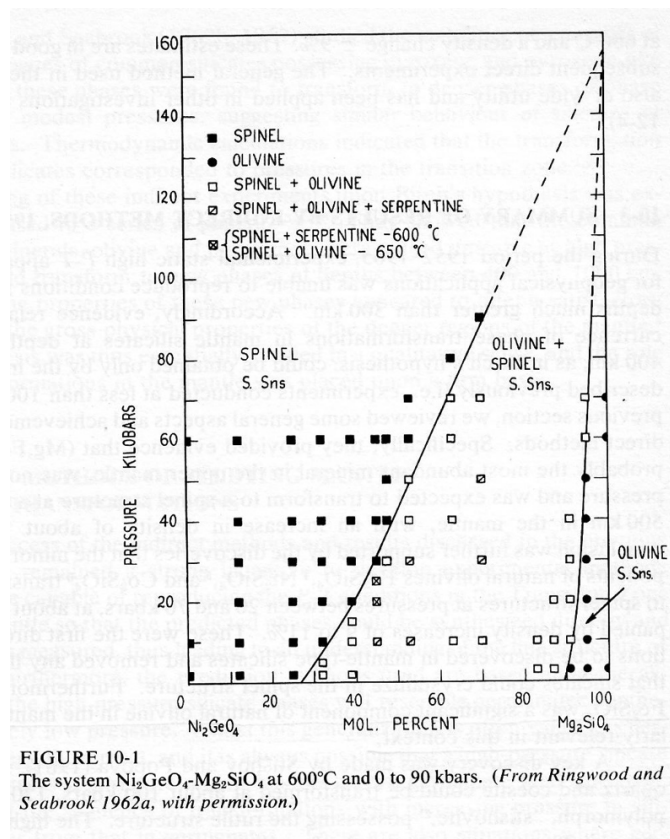
Olivine - Spinel transition hypothesis

Bernal. J. D. (1936)

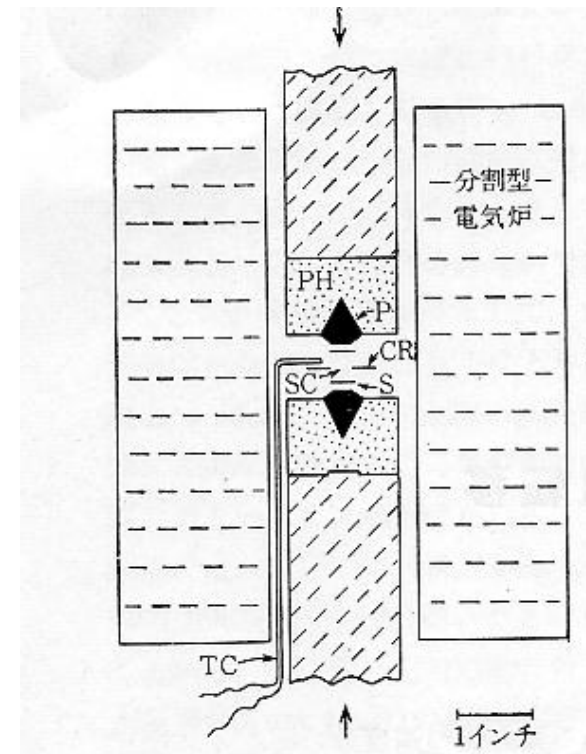
Jeffery H. (1937)

Experimental proof of Olivine-Spinel transition (I)

Ringwood (1958) Fe_2SiO_4 , 600°C, 38 kbar



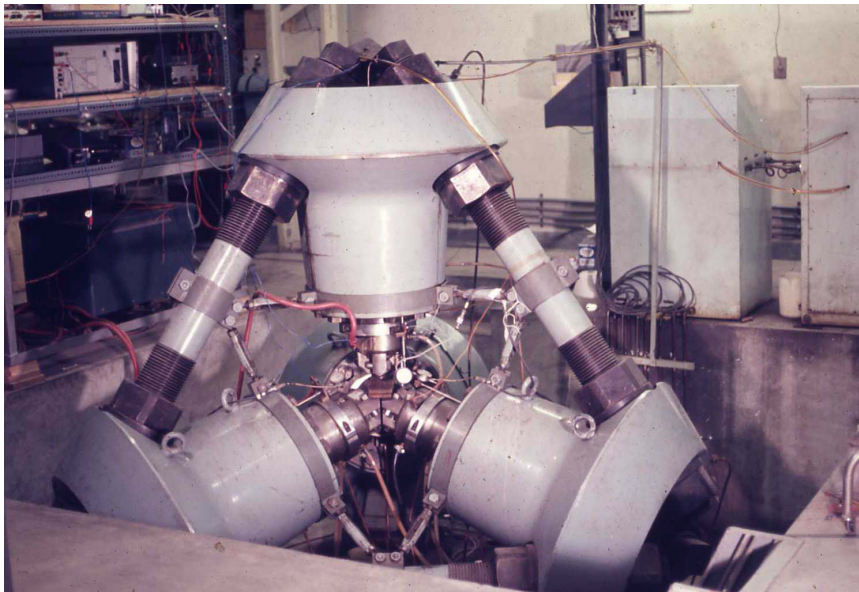
Ni_2SiO_4 - Mg_2SiO_4 system



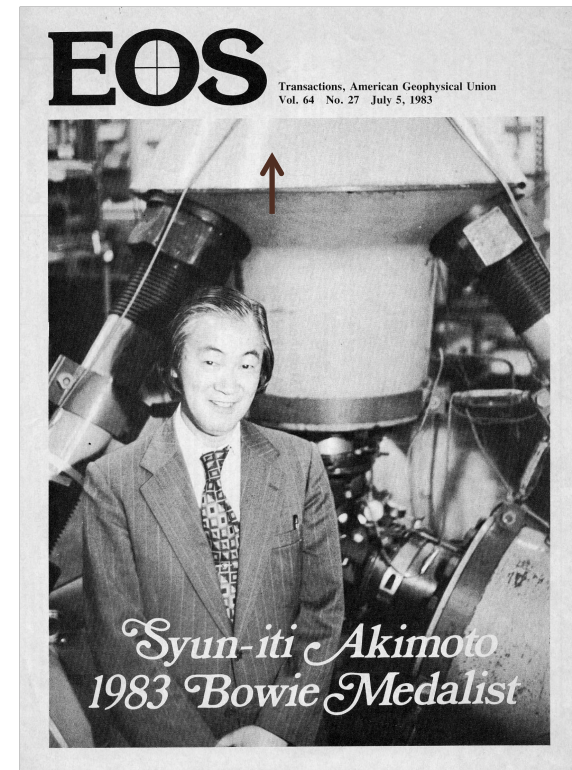
(simple squeezer apparatus)

Experimental proof of Olivine-Spinel transition (II)

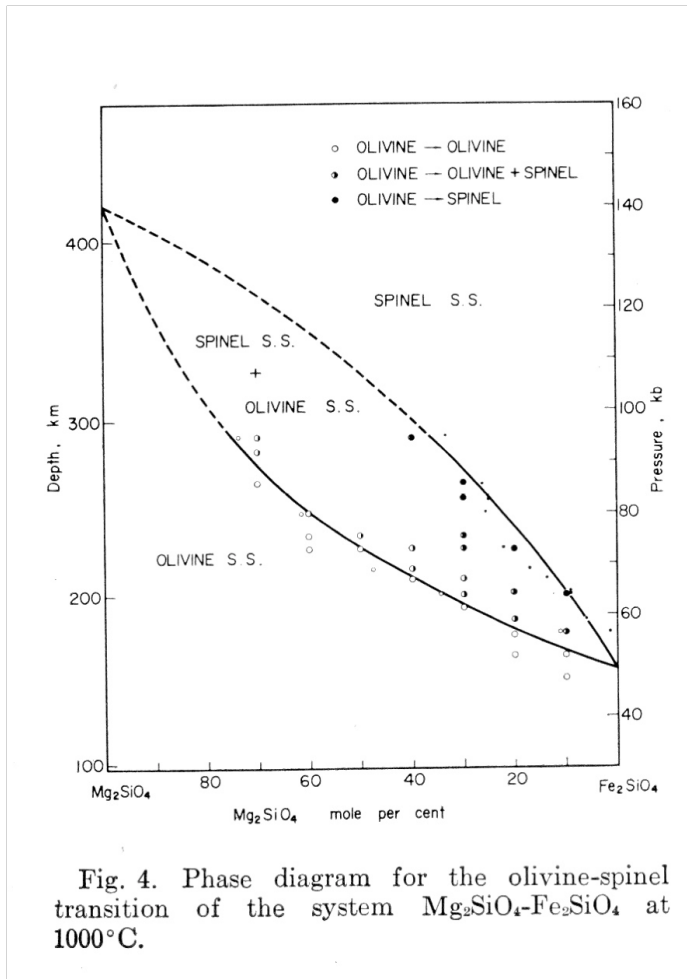
Akimoto (1963)



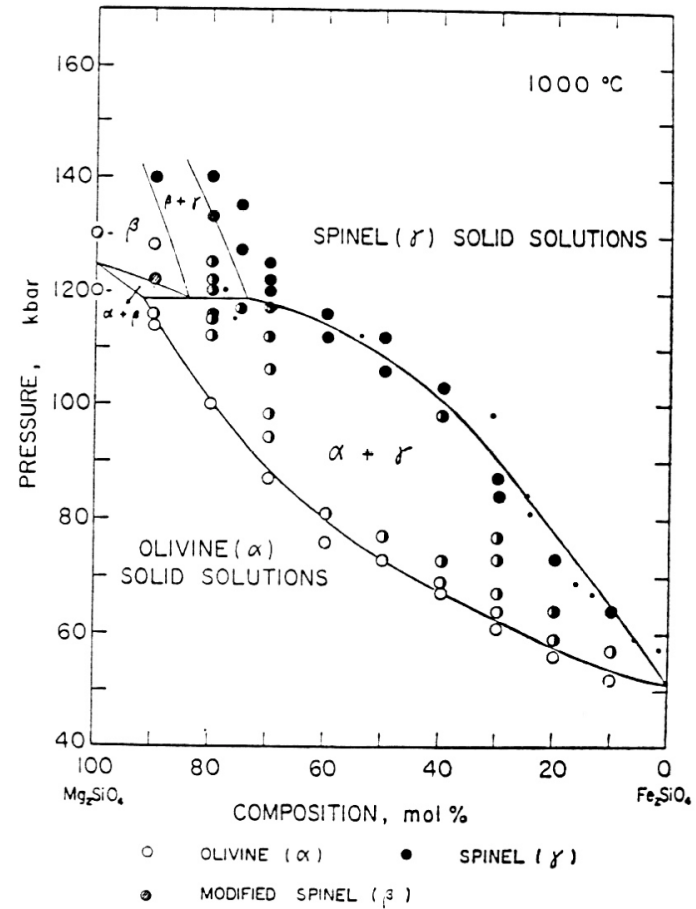
Tetrahedral press at ISSP



Detailed study of Olivine-Spinel transition

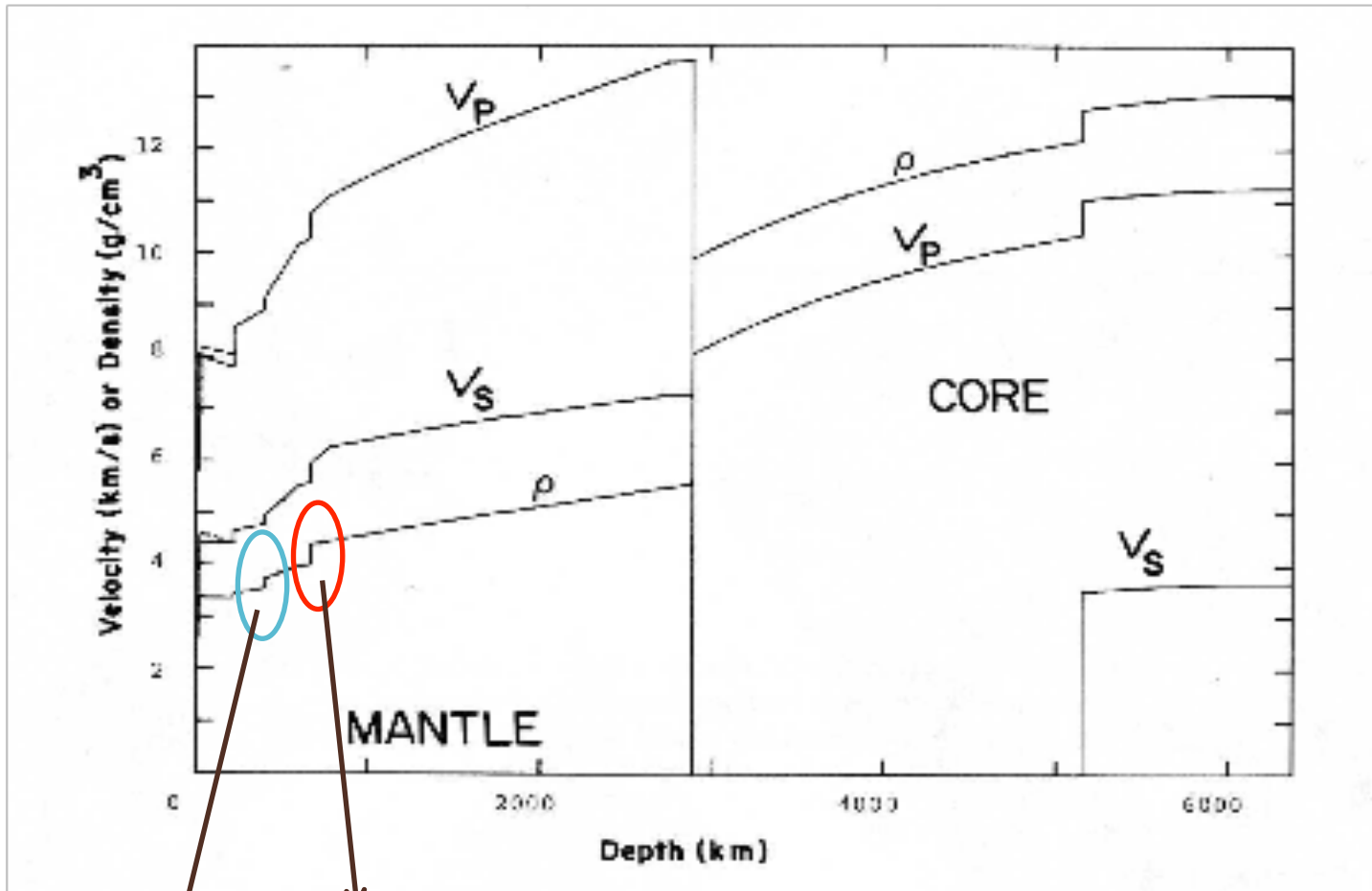


Akimoto & Fujisawa (1968)



Akimoto et al. (1972)

Seismic Discontinuities in the Mantle



660 km : spinel → "post spinel transition" ?
410 km : olivine → spinel

Origin of the 660 km Discontinuity

Possibilities for the “post-spinel phase”

A_2BO_4 with denser structure

(K_2NiF_4 type, Sr_2PbO_4 type, ...)

$ABO_3 + AO$

(ilmenite, perovskite, corundum) + rocksalt

$2AO + BO_2$

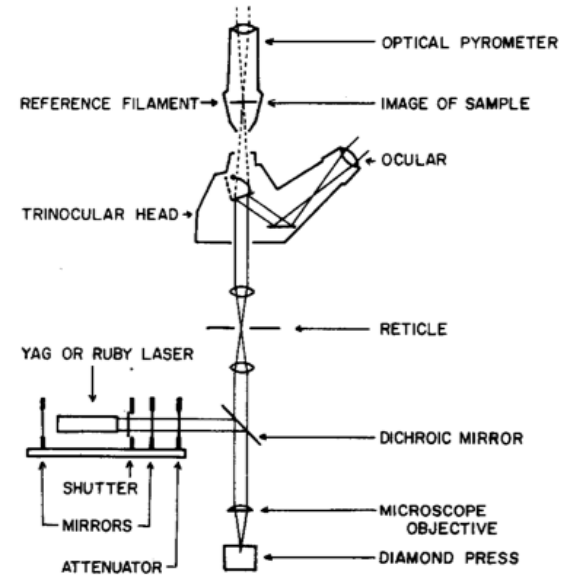
rocksalt + rutile

Finding of Silicate Perovskite

Liu (1974)

“silicate perovskite from garnet”

(laser heated diamond anvil)



perovskite (cation : anion = 2 : 3)

Origin of the 660 km Discontinuity

Possibilities for the “post-spinel phase”

A_2BO_4 with denser structure

(K_2NiF_4 type, Sr_2PbO_4 type, ...)

$ABO_3 + AO$

(ilmenite, perovskite, corundum) + rocksalt

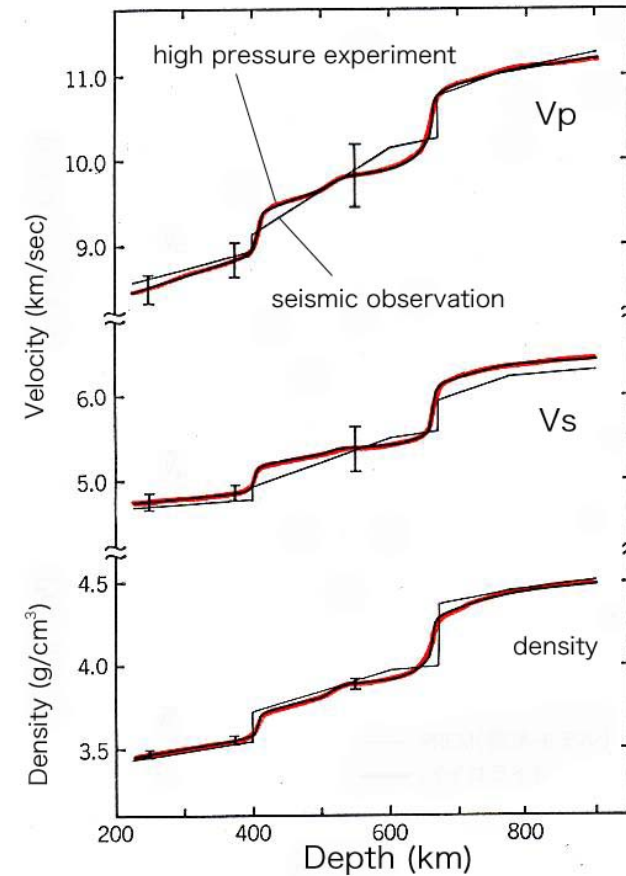
$2AO + BO_2$

rocksalt + rutile

Constitution of the mantle

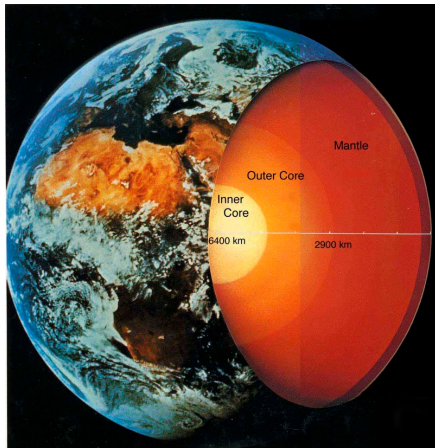
Upper mantle	Lower mantle
olivine	→ perovskite + rocksalt
pyroxene	→ perovskite
garnet	→ perovskite
(transition zone: spinel, ilmenite)	

Lower mantle : complicated solid solution
with perovskite structure

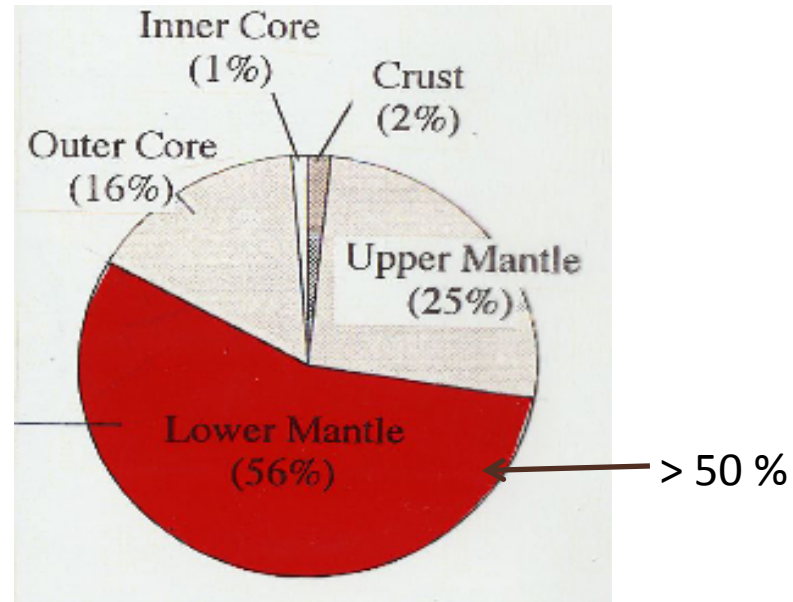


Comparison of calculated property
and seismic observation

“The most abundant mineral” of the Earth



Volume ratio of the Earth



Perovskite : the most abundant mineral of the Earth

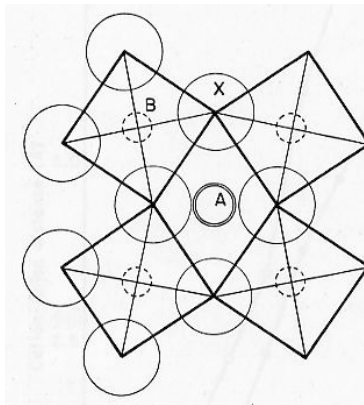
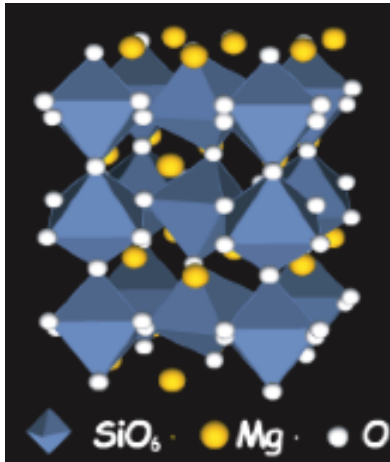
perovskite-type $(\text{Mg,Fe})\text{SiO}_3$

mineral name : “bridgmanite” after P. W. Bridgman

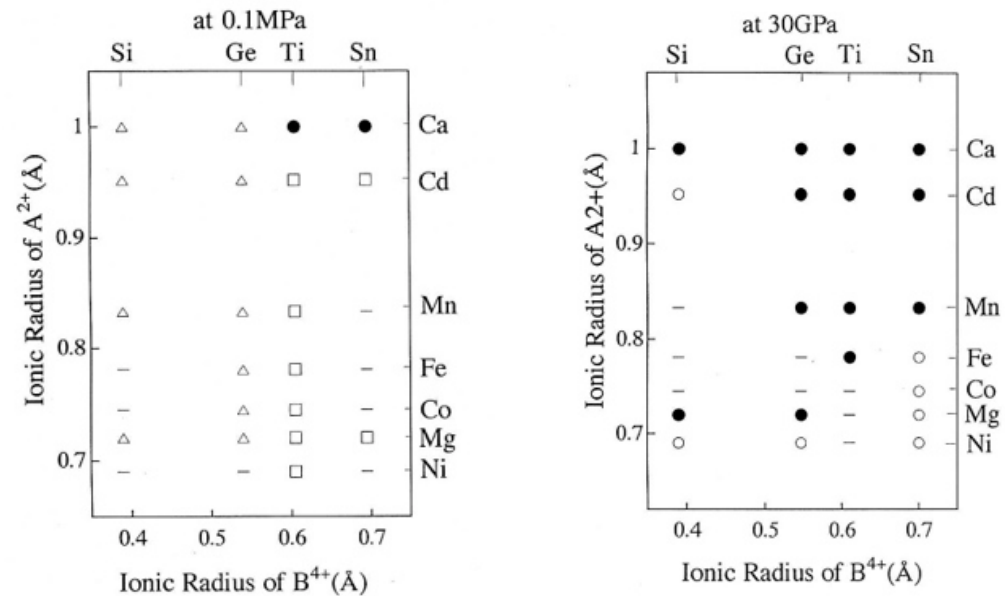
Crystal Structure of Silicate Perovskite

perovskite structure: fcc close packing of O and A cation

→ unusually dense packing



stable structures of ABO_3 -type compounds



● : perovskite

Stability of Silicate Perovskite

Experiments

Knittle and Jeanloz (1987) ; Experiments up to 127 GPa

“silicate perovskite is stable throughout the lower mantle”

Kesson et al. (1998) ; Experiments up to 135 GPa

“MgPv was found to be present and no additional phases or disproportionations were encountered”

Theoretical consideration

perovskite structure : ultimate dense form of ABO_3 -type compounds



perovskite is stable to the bottom of the mantle

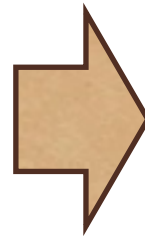
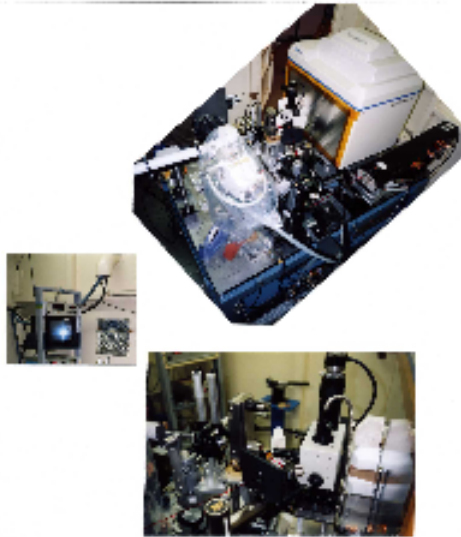
Construction of Laser Heated DAC combined with Synchrotron Radiation (I)

Big grant from the government (1995 - 1999)

“Study of the Structure and Properties of the Lower Mantle based on
High Pressure and High Temperature experiments”

Photon Factory BL-13

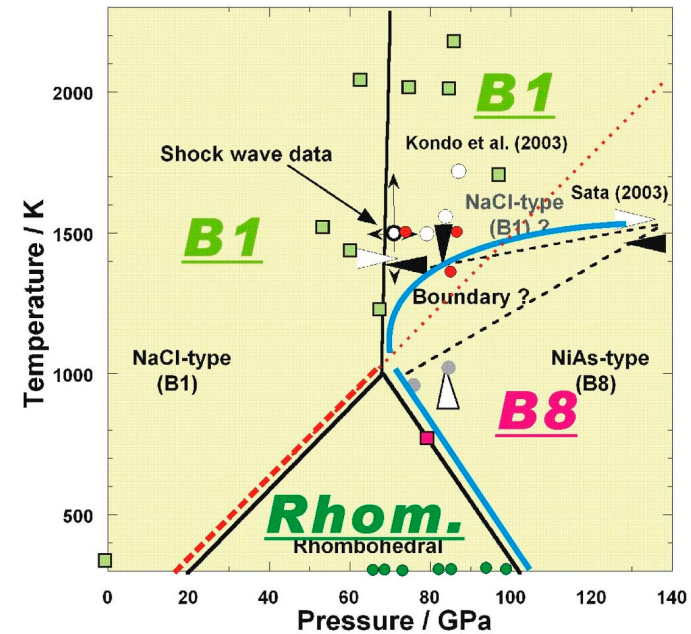
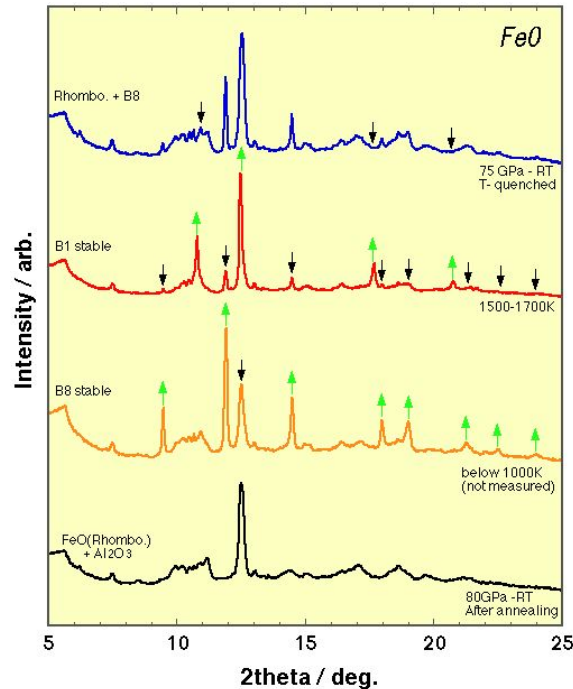
CO₂ laser



YAG laser



Study of the Minerals in the Lower Mantle



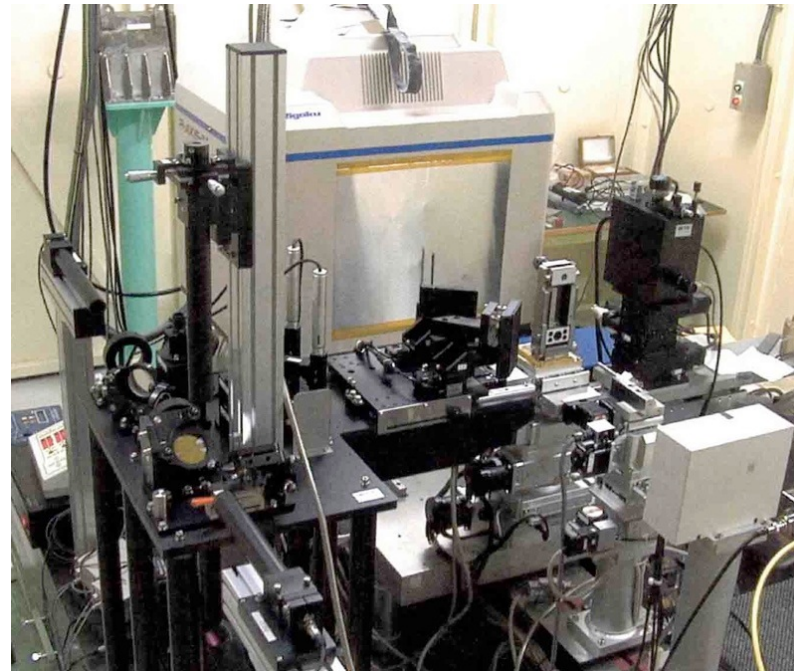
- Funamori et al. (1997) *Science* "Transformation in garnet from orthorhombic perovskite"
- Miyajima et al. (1999) *Phys. Earth Planet. Inter.* "Garnet-perovskite transformation"
- Kondo et al. (2000) *J. Appl. Phys.* "Phase transitions of MnO to 137 GPa."
- Miyajima et al. (2001) *Am. Mineral.* "Potential host phase of aluminum and potassium"
- Kondo et al. (2004) *Phys. Earth Planet. Inter.* "Phase transitions of (Mg, Fe)O at megabar....."

Construction of Laser Heated DAC combined with Synchrotron Radiation (II)

SPring-8



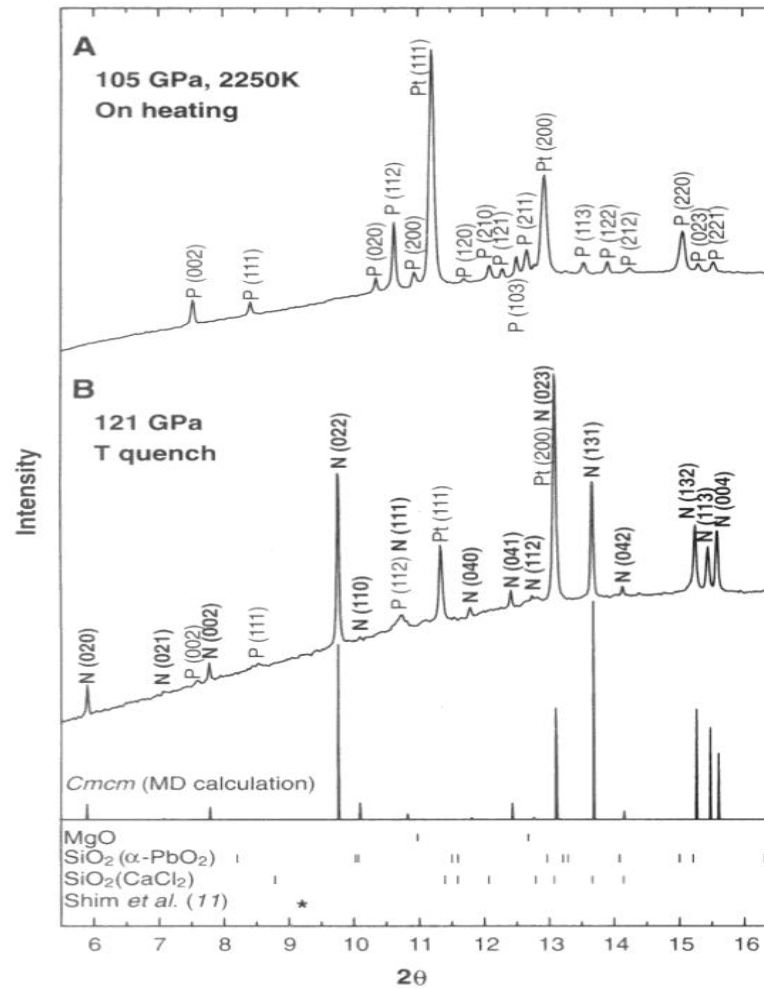
BL10-XU



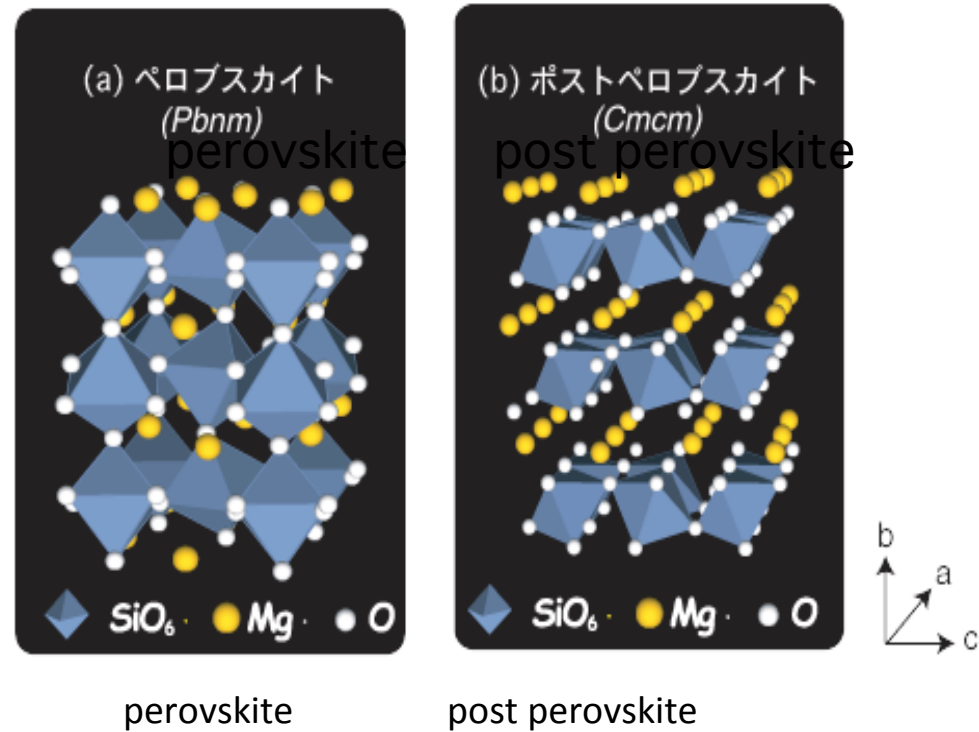
Finding of A New Phase in MgSiO₃

"Post-Perovskite Phase Transition in MgSiO₃"

Murakami et al., (2004)



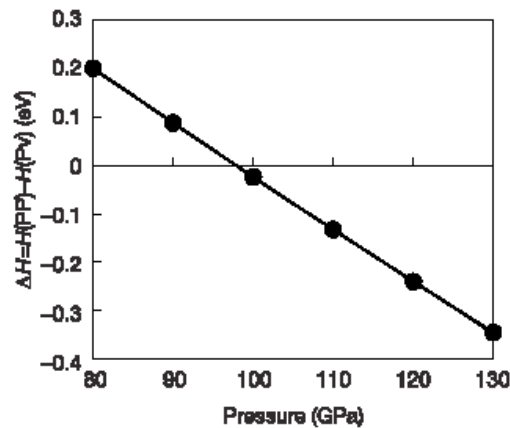
Structures of Perovskite and Post-perovskite



CaIrO_3 , AgTaS_3 , UFeS_3 , LaYbS_3 , UScS_3 , ThMnSe_3 , UMnSe_3 , CeYbSe_3 , ...
(high pressures ; MgGeO_3 , MnGeO_3 , ...)

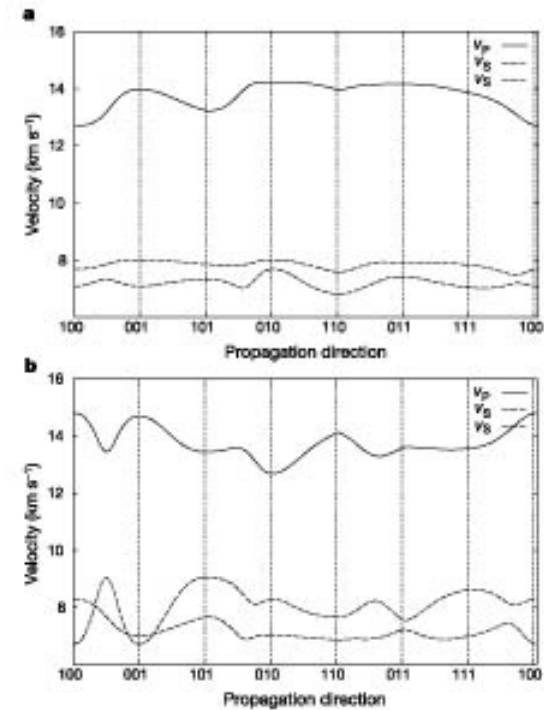
Theoretical Calculations of Stability and Elasticity (I)

First principle calculation



$$\Delta H = H(PP) - H(Pv) \text{ at } 0\text{K}$$

The elasticity of the MgSiO_3 post-perovskite phase in the Earth's lower mantle, T. litaka, et al., Nature, 430,442(2004)



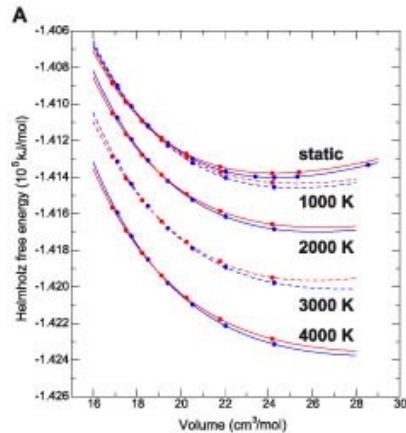
Pv

PP

Figure 3 The variation of compressional (v_p) and shear (v_s) wave velocities as a function of propagation direction: **a.** Perovskite phase at 100 GPa; **b.** post-perovskite phase at 100 GPa. The two dashed lines represent the two polarizations of the shear waves.

elasticity

Theoretical Calculations of Stability and Elasticity (II)



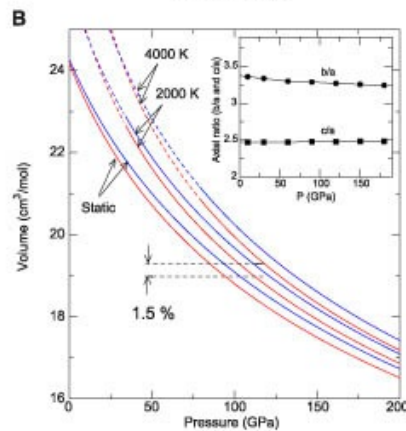
Observed unit cell



First principle calculation

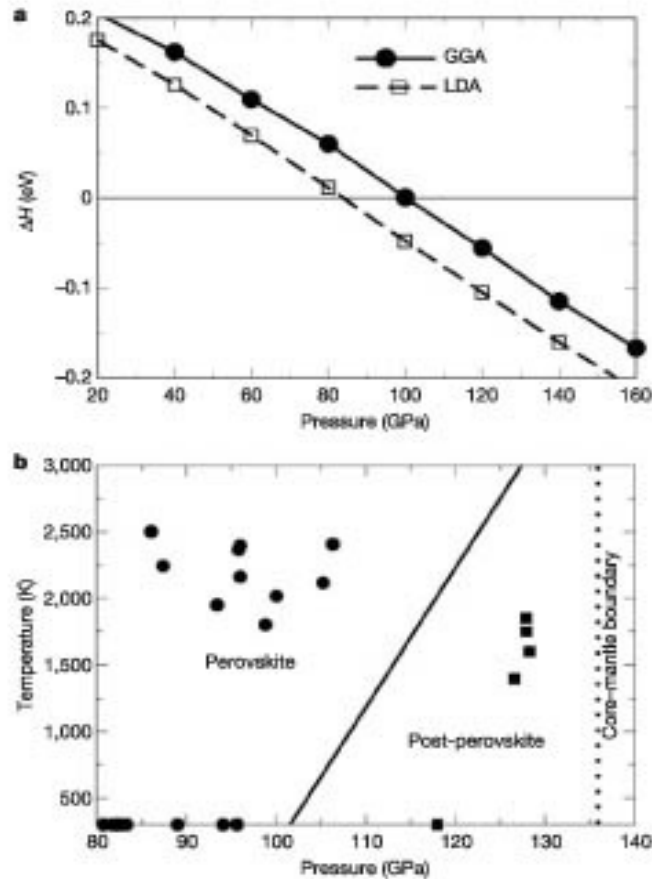


Post perovskite structure



Theoretical and experimental evidence for a post-perovskite phase of MgSiO₃ in Earth's D'' layer,
Tsuchiya et al., Earth Planet. Sci. Lett., 224, 241(2004)

Theoretical Calculations of Stability and Elasticity (III)



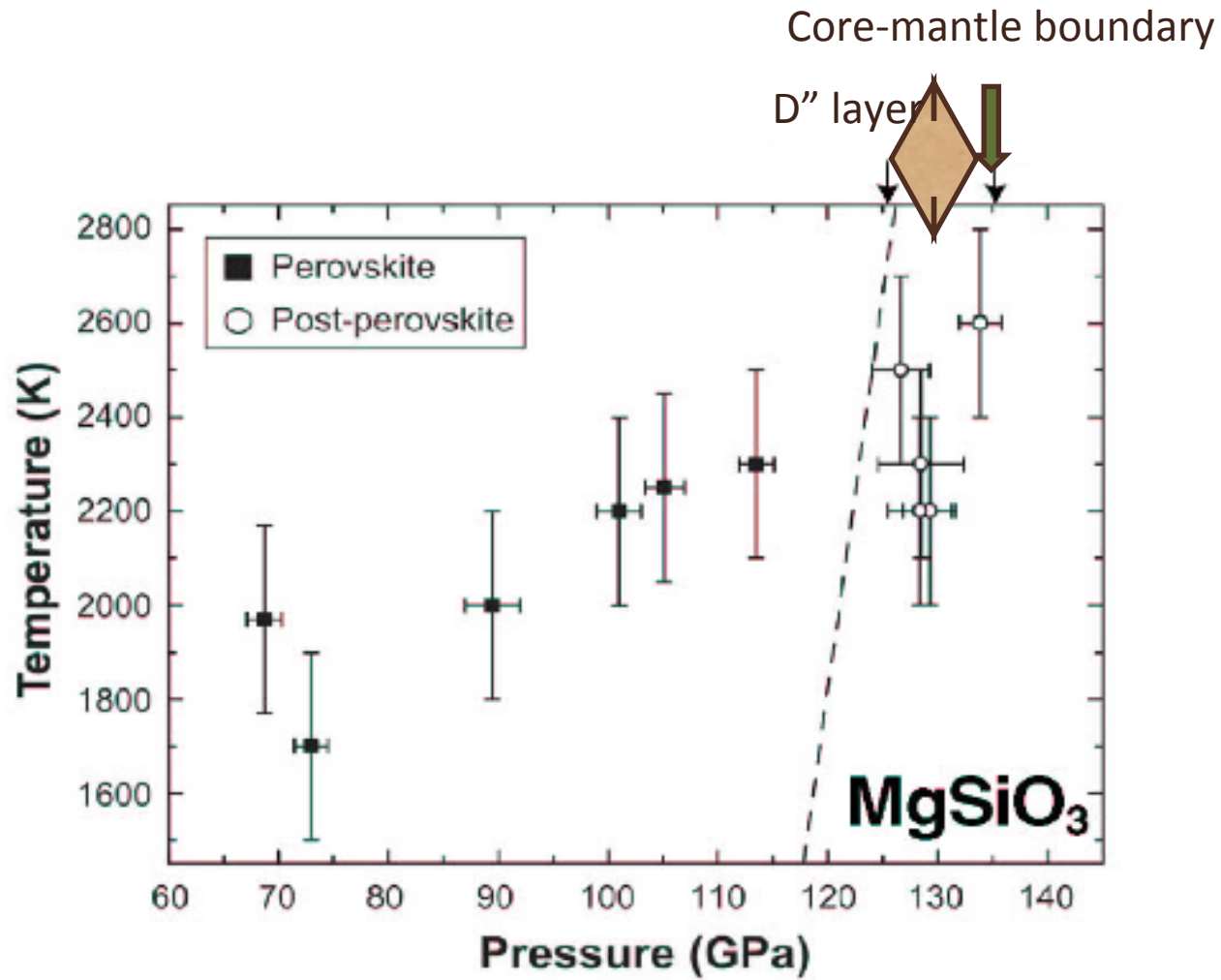
CaIrO_3 -type Cmcm structure

ab initio simulations based on density functional theory

Theoretical and experimental evidence for a post-perovskite phase of MgSiO_3 in Earth's D'' layer,

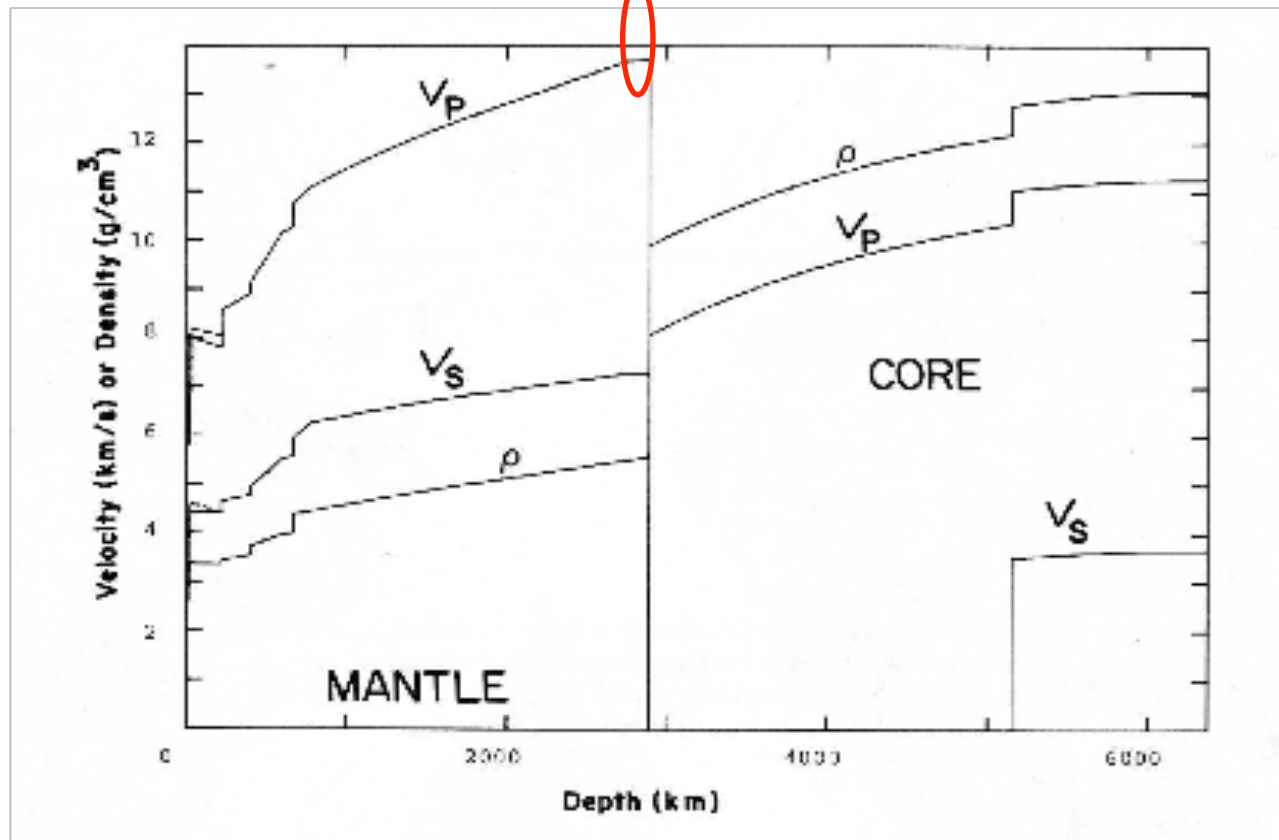
Oganov and Ono, Nature, (2004)

Stability Field of the New Phase



Seismic Discontinuities in the Mantle

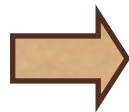
D'' layer



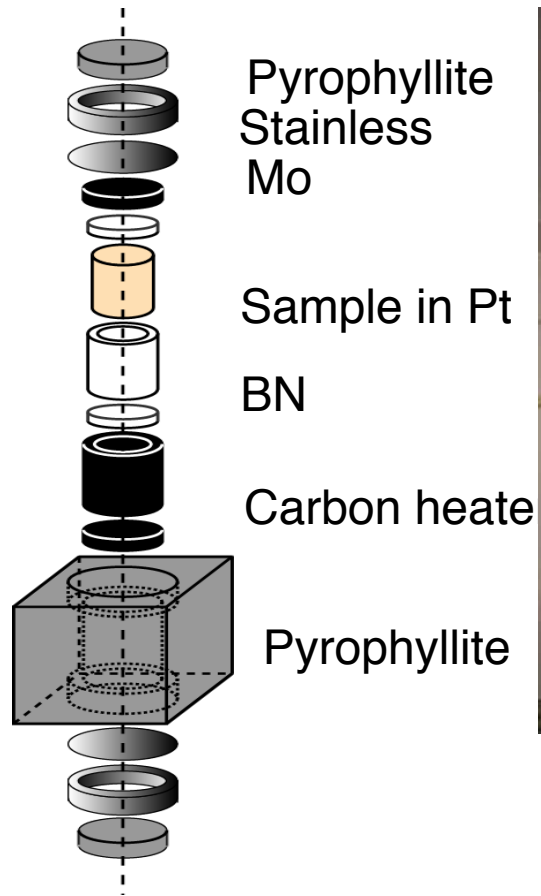
Property of Post-Perovskite Structure

Using CaIrO_3 as model material

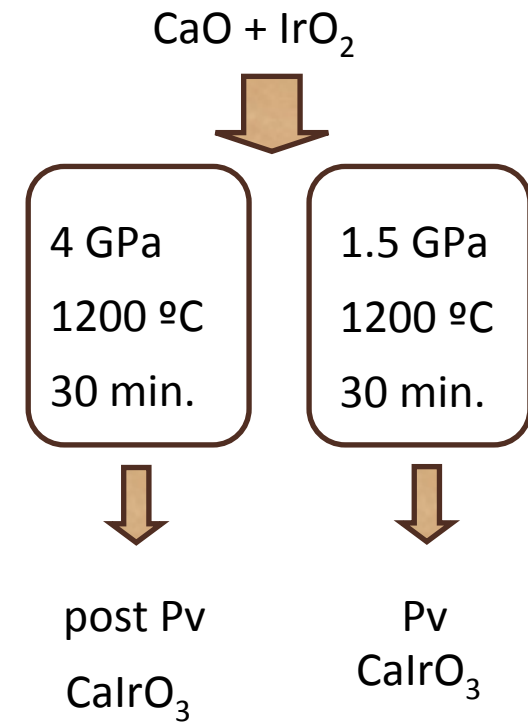
- MgSiO_3
formed only above 120 GPa
unquenchable to ambient condition
- CaIrO_3
formed much easily
keep its structure at ambient condition
TEM observation
rheological property



High pressure synthesis of CaIrO_3

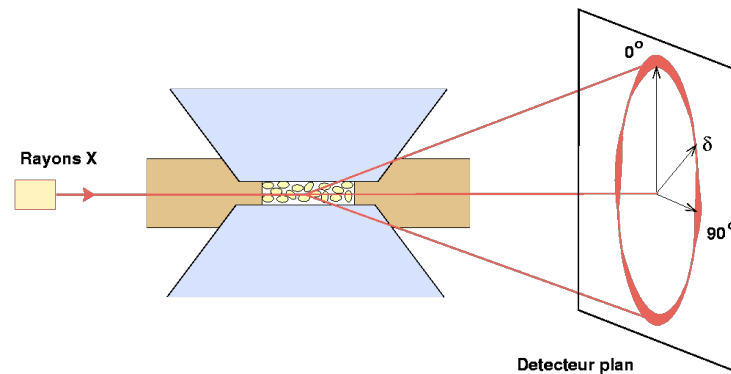
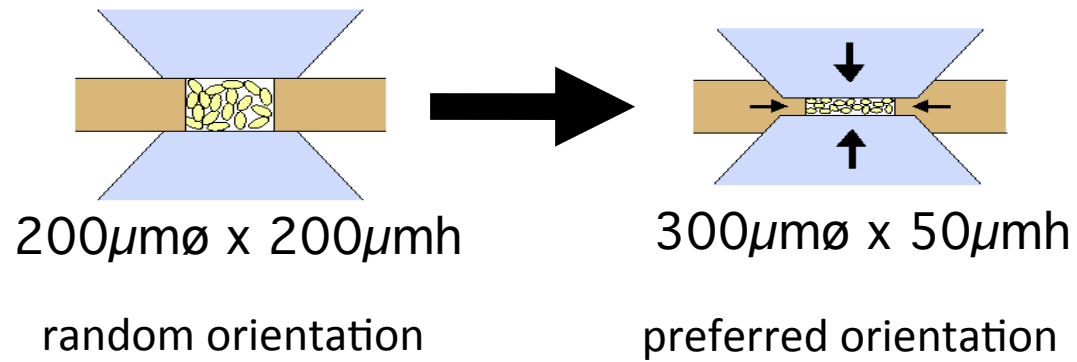


700 ton cubic press



Radial diffraction technique

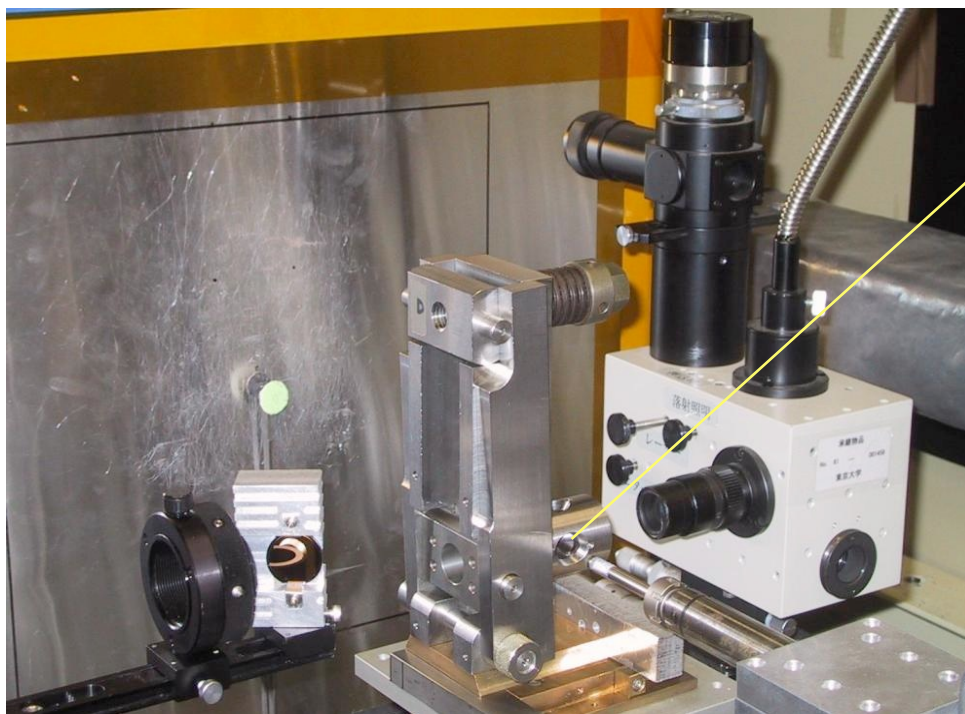
Large plastic deformation under uniaxial stress field



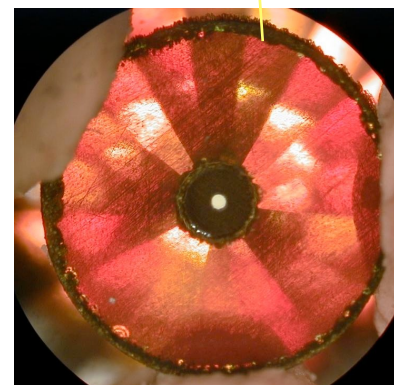
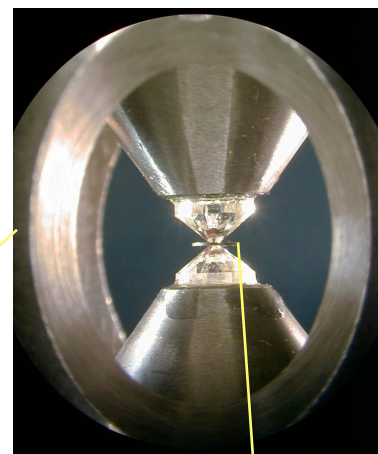
X-ray \perp compression axis

Radial diffraction experiment

Photon Factory BL13A



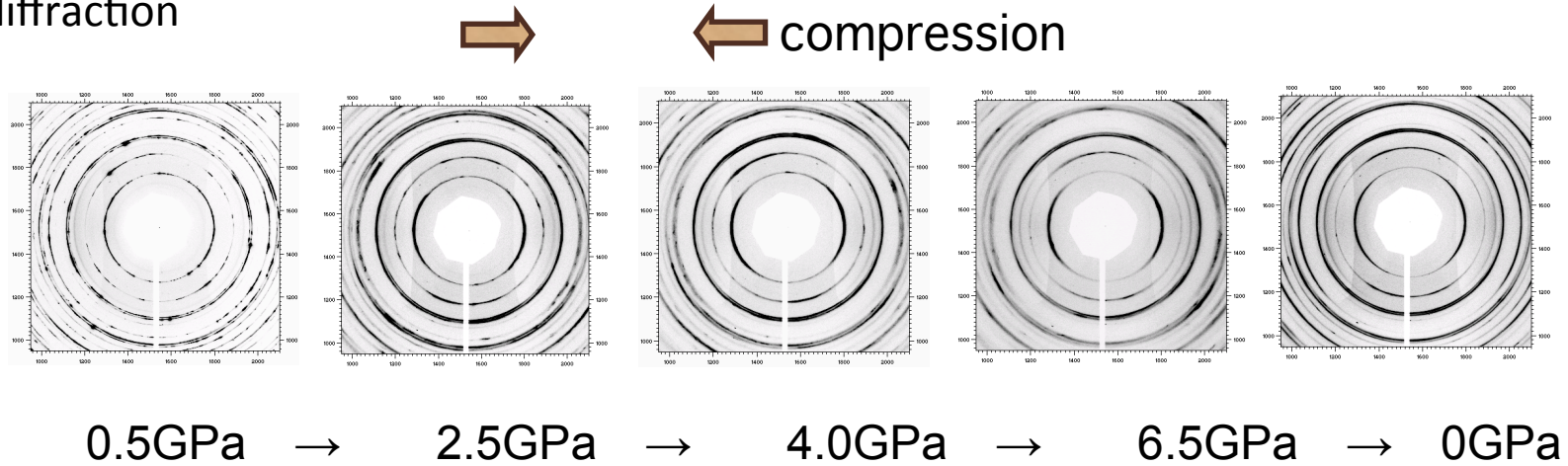
DAC with large side opening



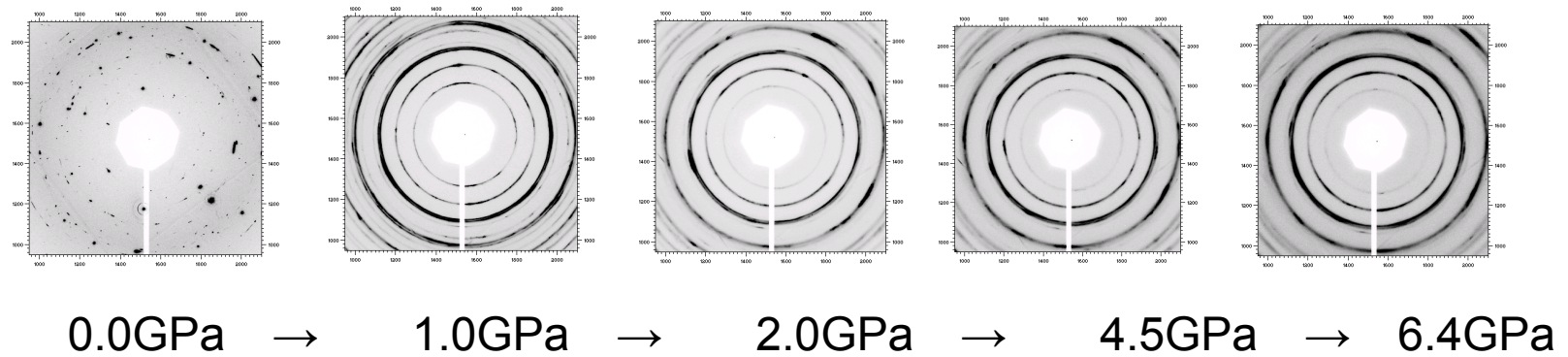
X-ray transparent gasket

Diffractions of post-perovskite phase

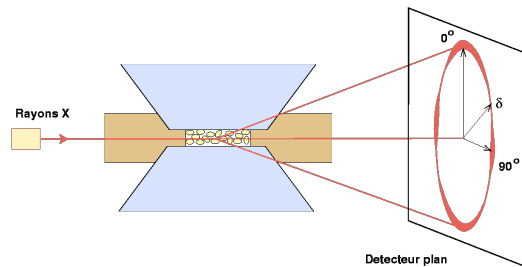
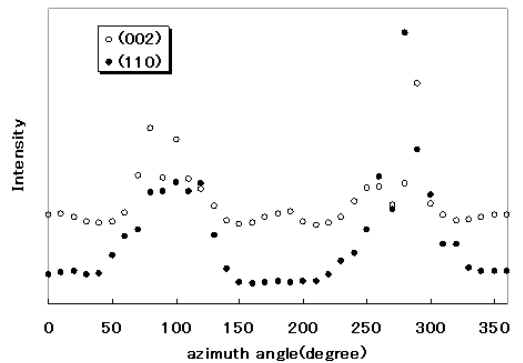
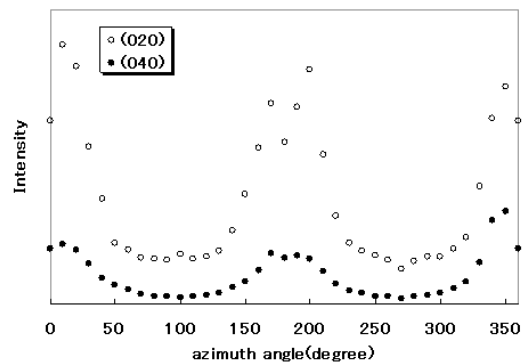
Radial diffraction



Axial diffraction



Lattice preferred orientation in pPv



$$b = 9.867 \text{ \AA}$$

$$a = 3.146 \text{ \AA}$$

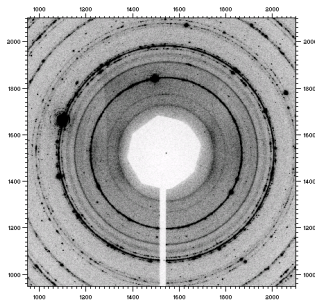
$$c = 7.298 \text{ \AA}$$

compression

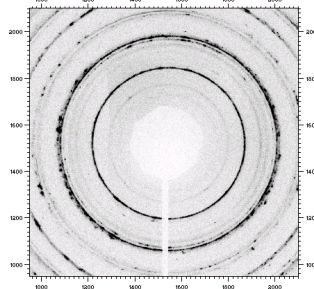
Radial diffraction of perovskite phase



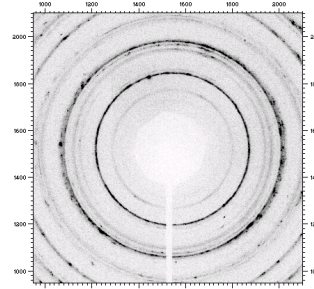
← compression



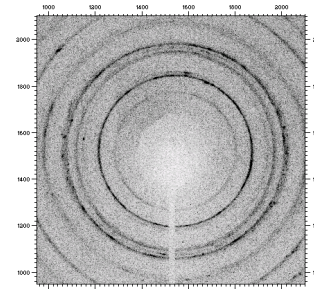
0GPa



1.6GPa

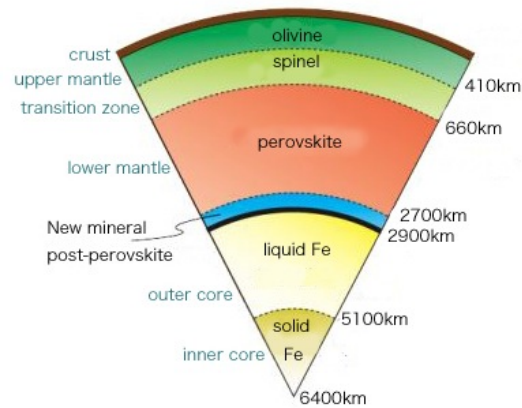


3.5GPa

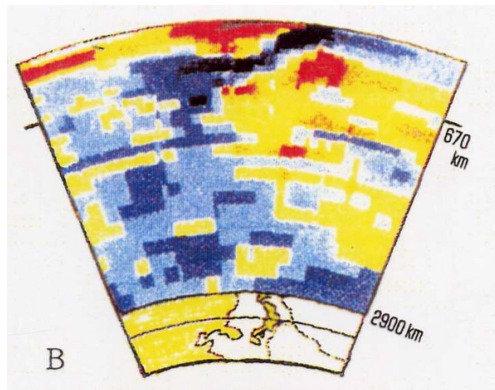


6.5GPa

Current view of the Earth - three dimensional dynamic model -

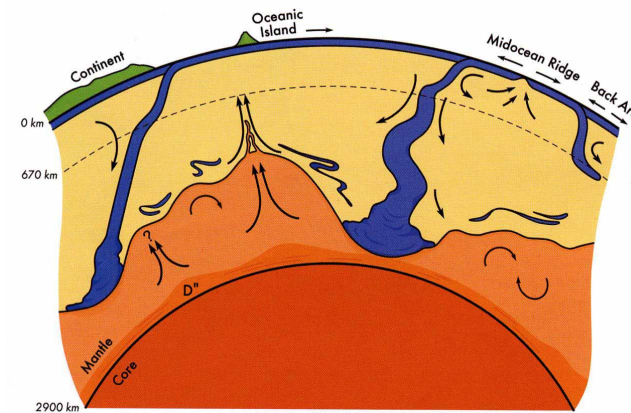


seismology

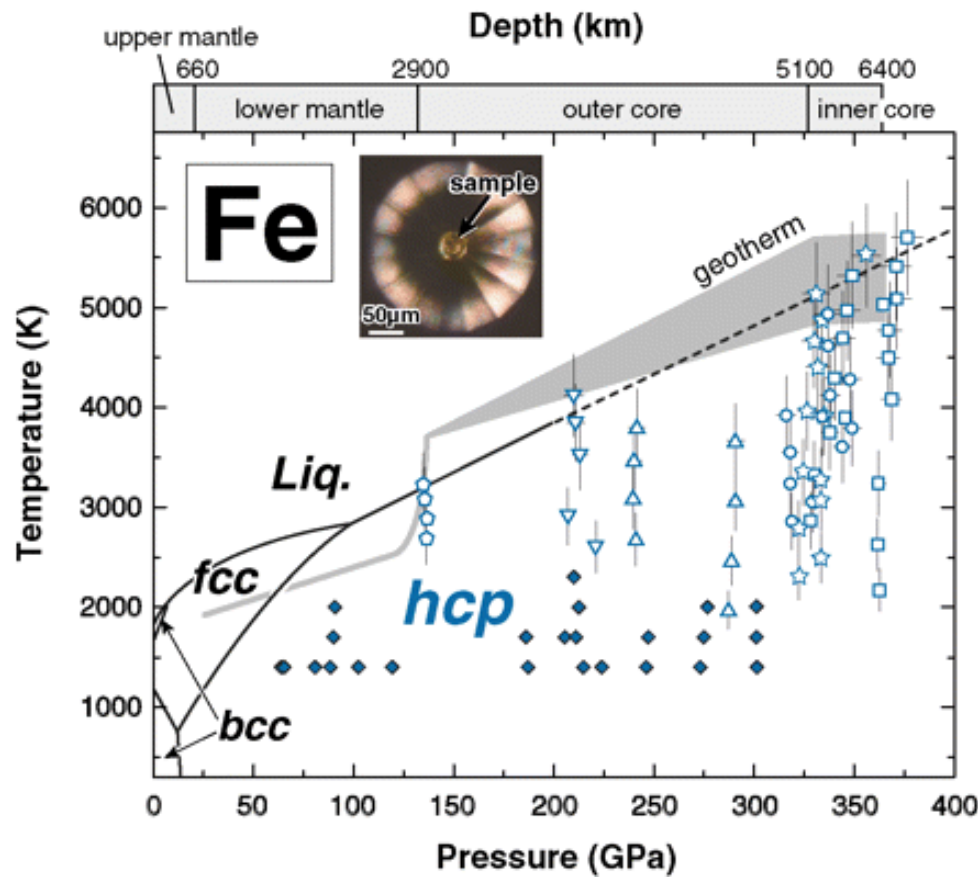


high P-T experiment

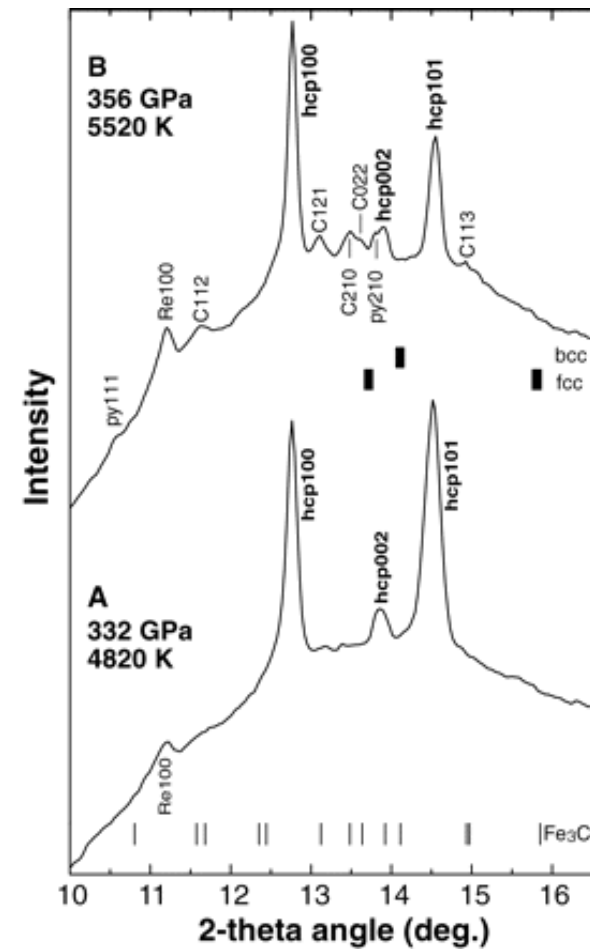
computer simulation



High P-T *in situ* experiments at the condition of the Earth's center



Tateno et al., *Science* (2010)

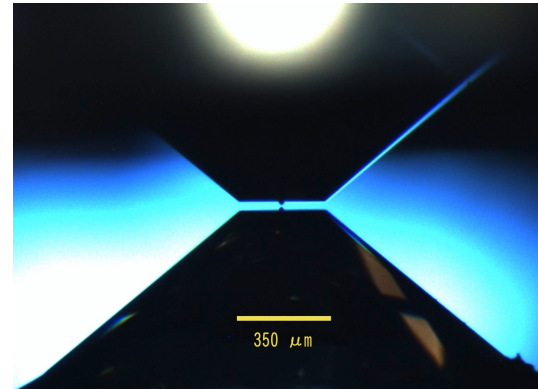


Beyond the center of the Earth

Micro diamond anvil fabricated by Focused Ion Beam (FIB) method

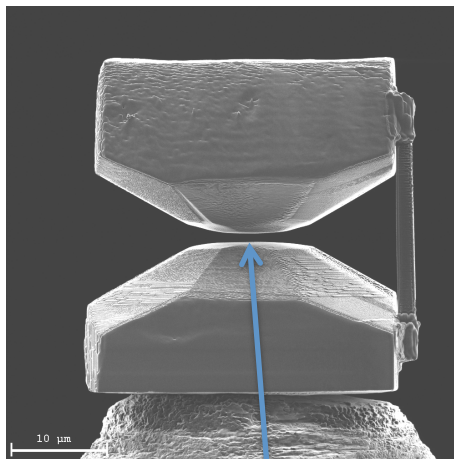


Culet diameter : 3 μm

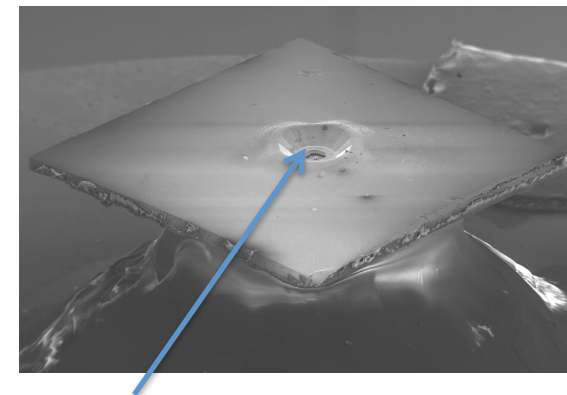
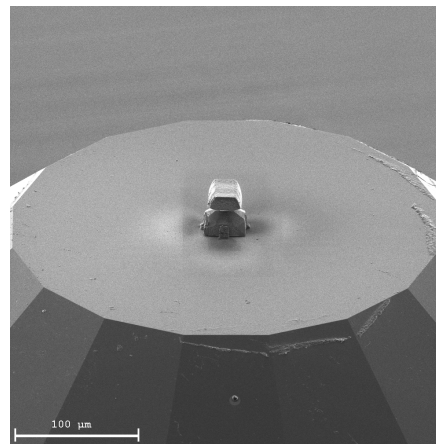


Micro anvils placed on top of normal anvils (350 μm culet)

“Micro paired-anvil”



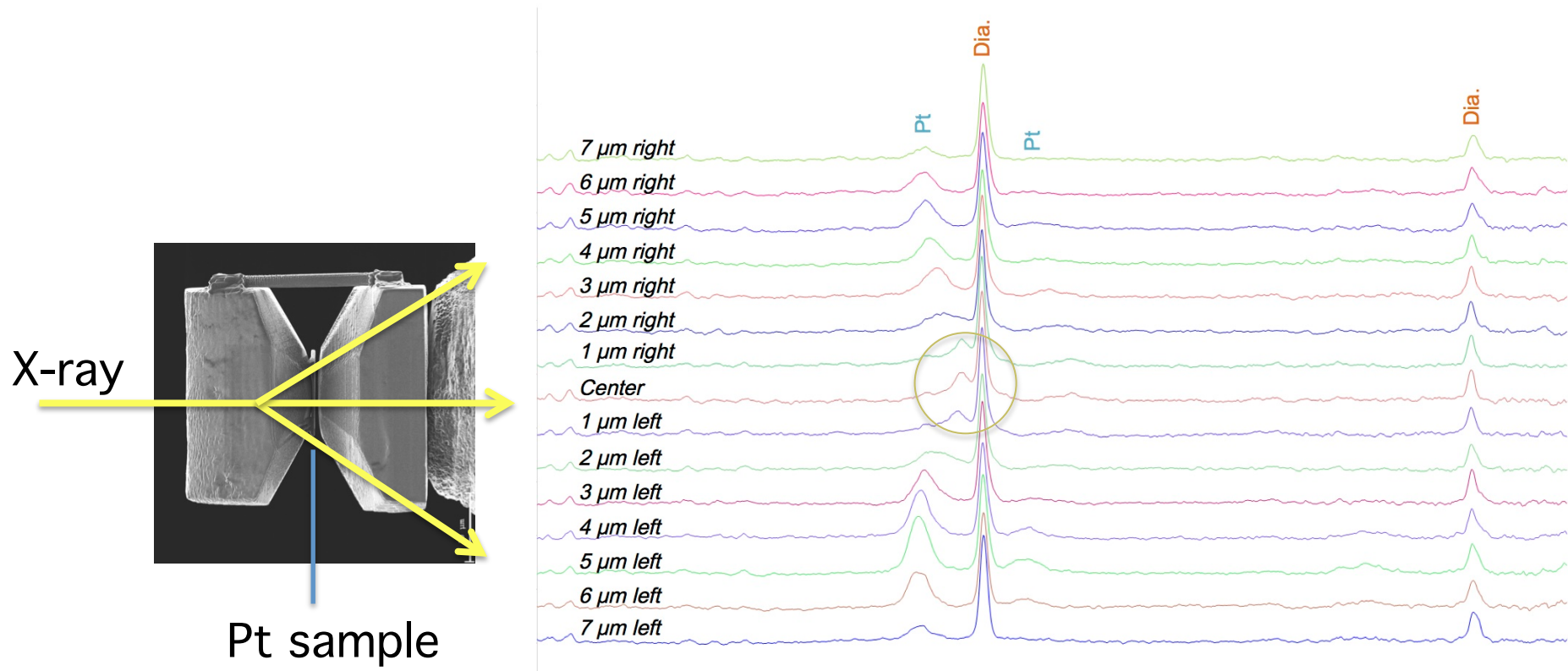
Put sample here



Gasket hole was filled with liquid

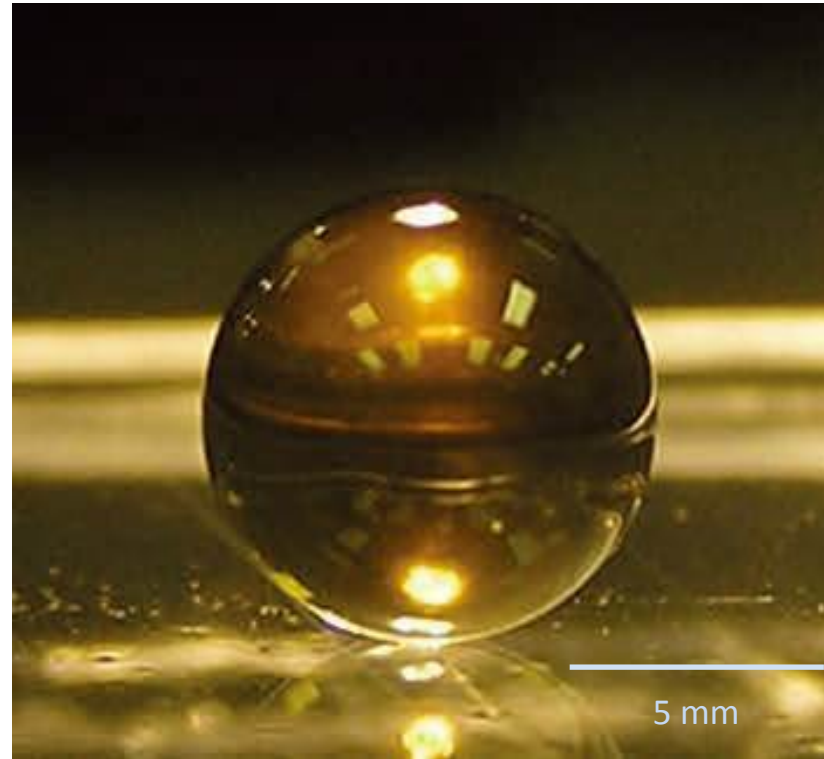
Sakai, Yagi, et al., *Rev. Sci. Instrum.* **86**, 033905 (2015)

Diffractions obtained by “1 μm ” beam at BL-10



Pressure of 426 GPa was achieved by this technique just recently.

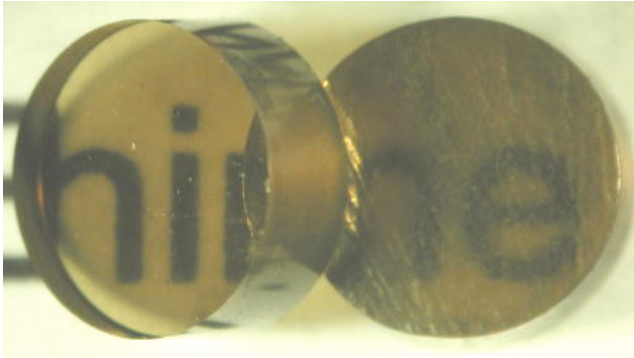
Application of high pressure techniques to the synthesis of new materials



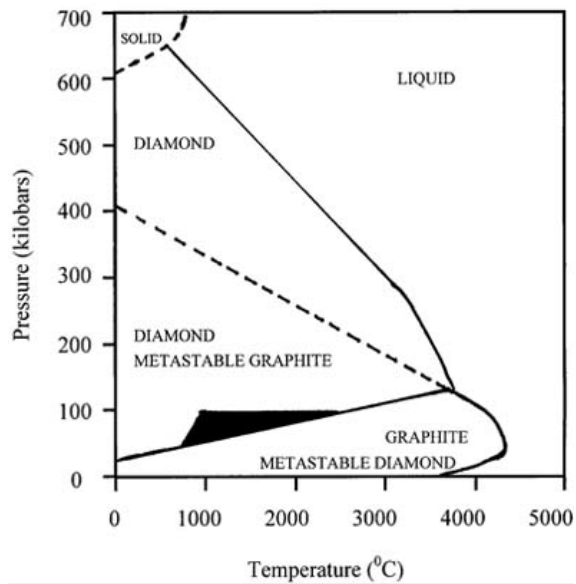
nano-polycrystalline diamond synthesized at 15 GPa

Irifune et al., (2013)

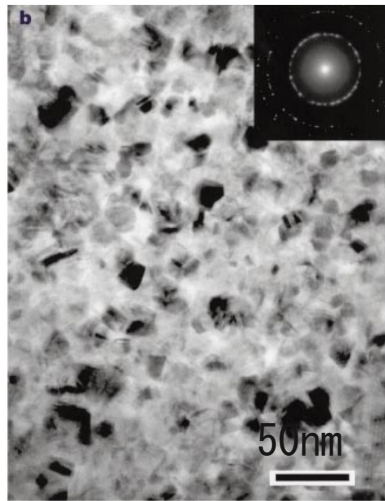
Synthesis of nano polycrystalline diamond



“Hime dia” synthesized at 15GPa,2000K



Phase diagram of carbon



TEM image



6000 ton multi anvil press
(Ehime University)

Synthesis of nano polycrystalline stishovite

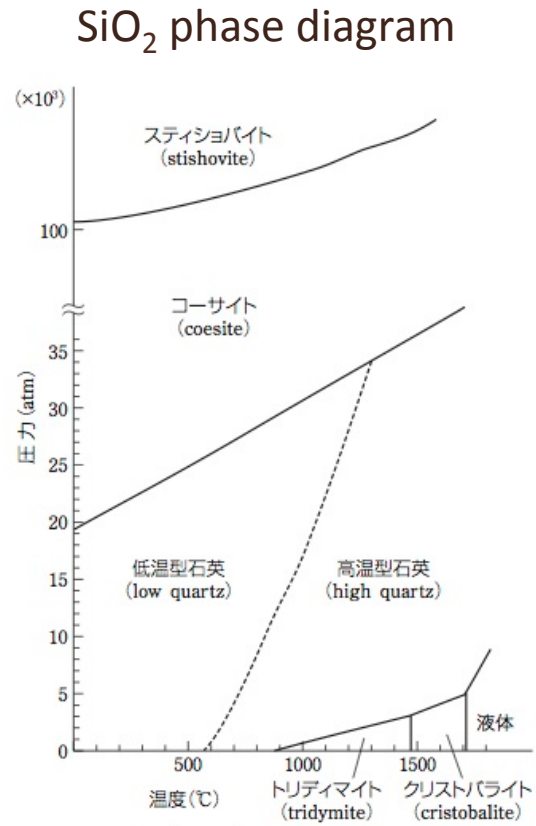
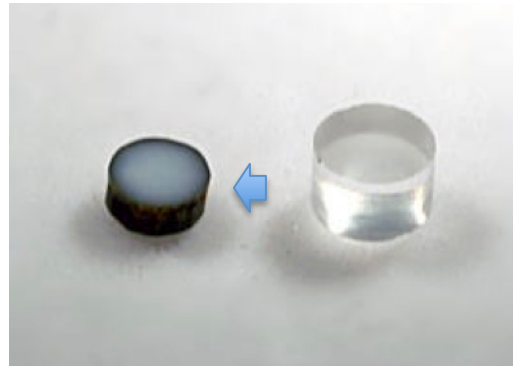
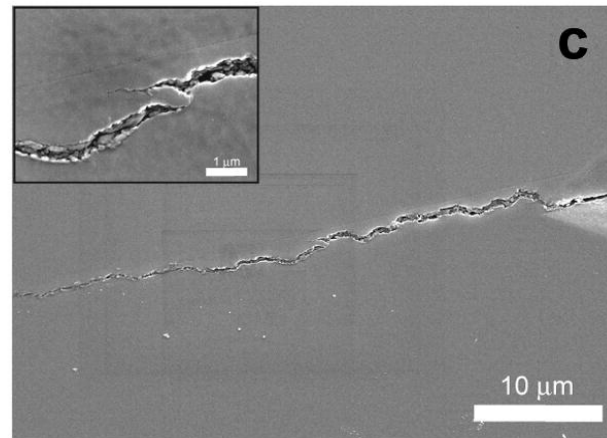
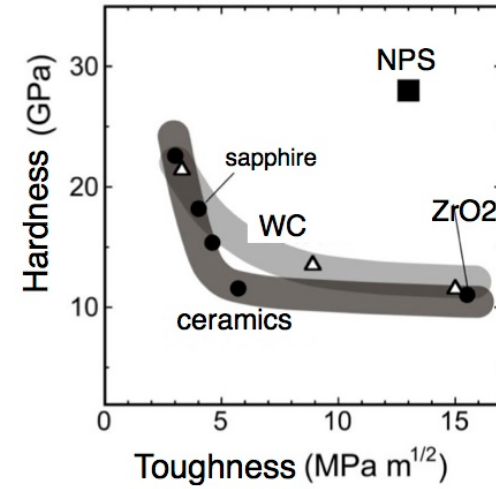


図3 SiO₂の相図(状態図)



NPS starting glass

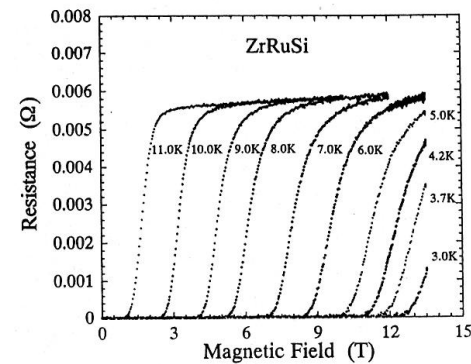
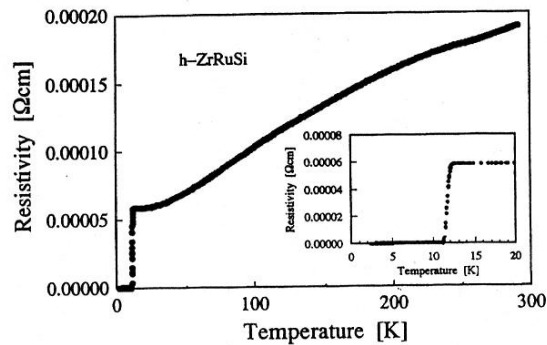


SEM observation of the crack

New super conductors synthesized under pressure

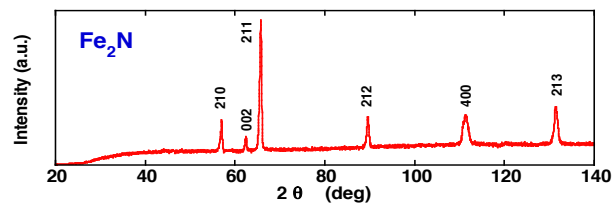
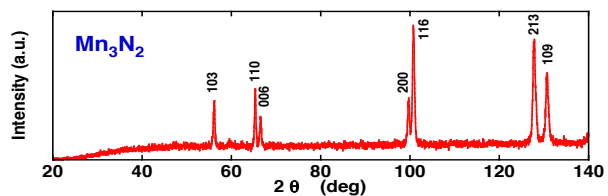
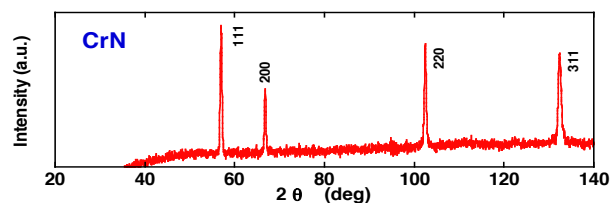
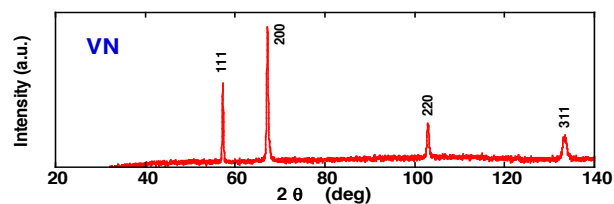
$T_c > 10$ K

material	T_c	structure
• ZrRuSi	12.2	Fe ₂ P-type
• ZrRuCe	10.5	TiFeSi-type
• ZrRu ₄ P ₂	11	ZrFe ₄ Si ₂ -type
• LaRu ₄ As ₁₂	10.3	skutterudite
• ZrRhSi	10.5	Co ₂ P-type

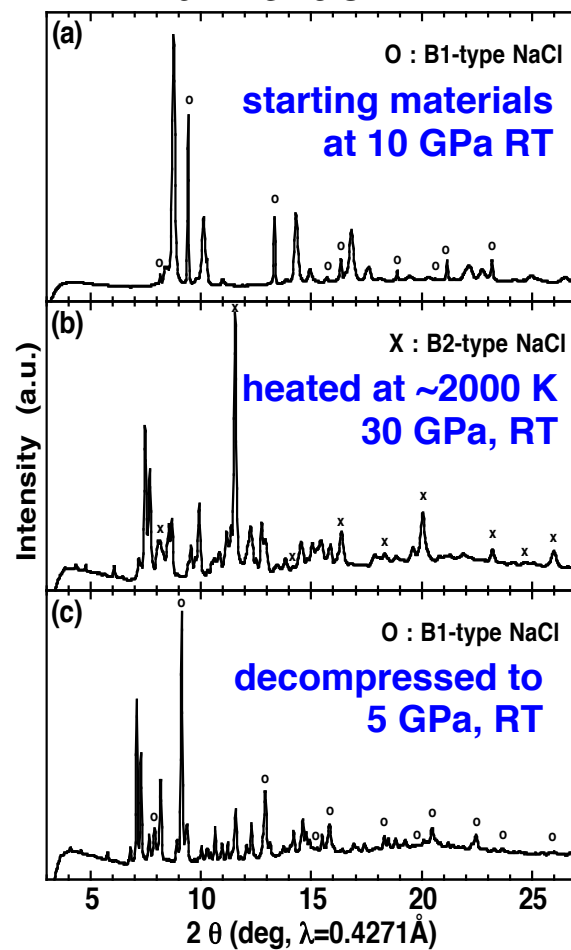


Synthesis of various nitrides

$P \sim 10$ GPa, $T \sim 1800$ K
transition metal nitride

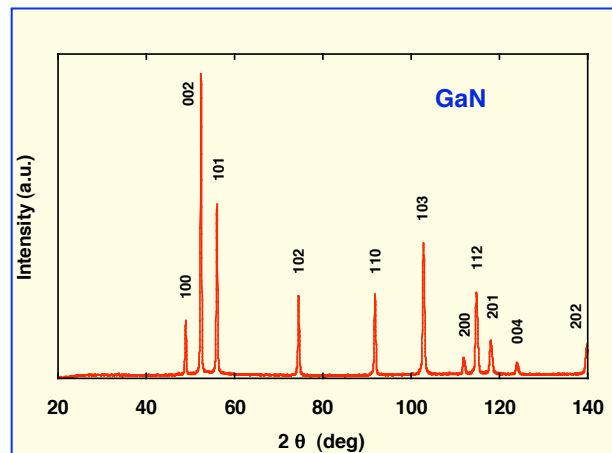
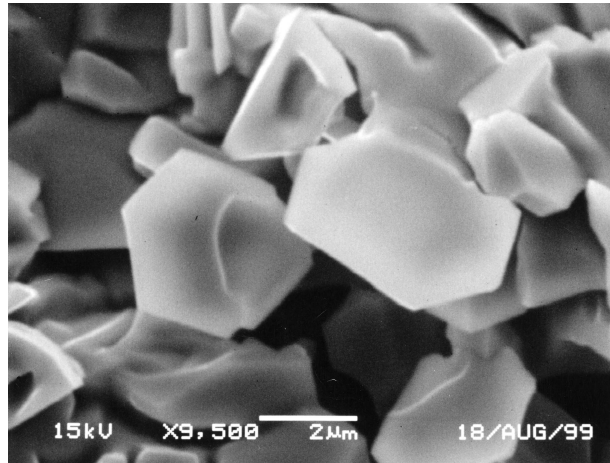


$P \sim 30$ GPa, $T \sim 2000$ K
La nitride



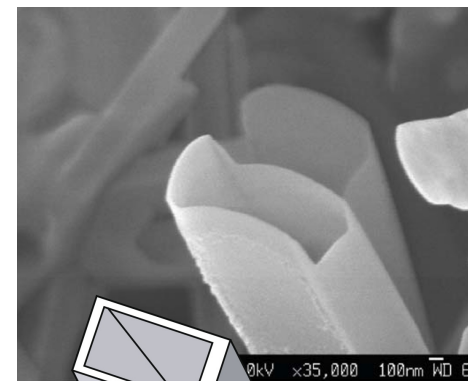
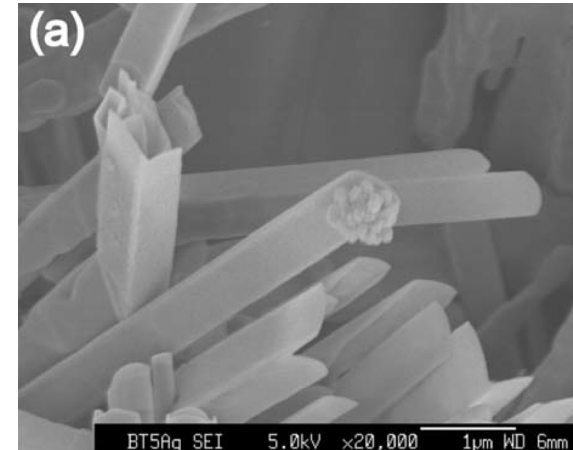
Synthesis of single crystals

GaN



(Hasegawa & Yagi, 2003)

GeO₂



(Niwa et al., 2009)

Summary

- High-pressure minerals in the Earth's deep interior were clarified through high-pressure and high-temperature X-ray experiments.
- High P & T *in situ* X-ray diffraction study is now possible at the condition corresponding to the center of the Earth.
- Further efforts are made to extend the pressure ranges beyond the center of the Earth
- Experimental techniques developed for such studies are now applied to make new novel materials.